

REGULARIZED D-BAR METHOD FOR THE INVERSE CONDUCTIVITY PROBLEM

KIM KNUDSEN, MATTI LASSAS, JENNIFER L. MUELLER, AND SAMULI SILTANEN

ABSTRACT. A strategy for regularizing the inversion procedure for the two-dimensional D-bar reconstruction algorithm based on the global uniqueness proof of Nachman [Ann. Math. **143** (1996)] for the ill-posed inverse conductivity problem is presented. The strategy utilizes truncation of the boundary integral equation and the scattering transform. It is shown that this leads to a bound on the error in the scattering transform and a stable reconstruction of the conductivity; an explicit rate of convergence in appropriate Banach spaces is derived as well. Numerical results are also included, demonstrating the convergence of the reconstructed conductivity to the true conductivity as the noise level tends to zero. The results provide a link between two traditions of inverse problems research: theory of regularization and inversion methods based on complex geometrical optics. Also, the procedure is a novel regularized imaging method for electrical impedance tomography.

Revised manuscript, September 22, 2009

Keywords: inverse problem, ill-posed problem, electrical impedance tomography, inverse conductivity problem, regularization

1. INTRODUCTION

We present a direct regularized reconstruction method for the nonlinear scalar inverse conductivity problem in dimension two. We prove that the method is a nonlinear regularization strategy in appropriate Banach spaces, introduce an admissible choice of regularization parameter, and derive an explicit estimate for the rate of convergence. Furthermore, we demonstrate the method computationally using simulated noisy impedance tomography data. Our results provide a link between two traditions of inverse problems research: theory of regularization and inversion methods based on complex geometrical optics.

Our algorithm particularly applies to electrical impedance tomography (EIT), which is an emerging medical imaging technique, as well as a method for subsurface geophysical imaging, and nondestructive industrial testing. An overview of applications with references can be found in [18]. The 2-D problem posed here is useful in imaging cross-sections of a region, such as a patient's chest. Medical applications include, but are not limited to, detecting regional aeration changes in the lung [24, 58, 59, 90], monitoring artificial ventilation [12, 24, 26, 90], monitoring pulmonary perfusion [12, 25, 73, 84], detecting extravascular lung water, [60], and evaluating shifts in lung fluid in congestive heart failure patients [21, 92].

For simplicity we let $\mathbb{D} \subset \mathbb{R}^2$ be the open unit disc; this is not a significant loss of generality as a large class of more general settings can be reduced to this case. Assume that $\gamma \in L^\infty(\mathbb{D})$ is real-valued and satisfies $\gamma(x) \geq c > 0$ for almost

every $x \in \mathbb{D}$ and that $\gamma \equiv 1$ in a neighborhood of $\partial\mathbb{D}$. We consider the generalized Laplace's equation

$$(1.1) \quad \nabla \cdot \gamma \nabla u = 0 \quad \text{in } \mathbb{D}, \quad u|_{\partial\mathbb{D}} = f,$$

with boundary measurements modeled by the Dirichlet-to-Neumann (DN) map

$$\Lambda_\gamma f = \gamma \frac{\partial u}{\partial \nu} \Big|_{\partial\mathbb{D}},$$

where $u \in H^1(\mathbb{D})$ is the solution to (1.1). It is well-known that Λ_γ is a bounded linear operator from $H^{1/2}(\partial\mathbb{D})$ to $H^{-1/2}(\partial\mathbb{D})$. Physically, u is the electric potential in \mathbb{D} , and Λ_γ represents knowledge of the current flux through $\partial\mathbb{D}$ resulting from any voltage distribution f applied on $\partial\mathbb{D}$.

The inverse conductivity problem posed by Calderón [17] is the problem of determining whether a strictly positive $\gamma \in L^\infty(\mathbb{D})$ is uniquely determined by Λ_γ and calculating γ in terms of Λ_γ if possible. An affirmative answer to Calderón's question, together with a calculation procedure for γ , was given by Astala and Päivärinta in [1].

In practical applications of the inverse conductivity problem the starting point is not the infinite-precision data Λ_γ ; only an approximate operator $\Lambda_\gamma^\varepsilon$ is available due to random noise and the necessarily finite number of measurements. The nonlinear inverse problem of reconstructing γ from boundary measurements is severely ill-posed (sensitive to measurement errors), and regularized inversion is needed.

We introduce in this work a regularized reconstruction method for twice differentiable conductivities based on Nachman [71]. The proof involves complex geometric optics (CGO) solutions, and therefore the Faddeev Green's function [23] (defined in the sense of tempered distributions)

$$(1.2) \quad G_k(x) := e^{ikx} g_k(x), \quad g_k(x) := \frac{1}{(2\pi)^2} \int_{\mathbb{R}^2} \frac{e^{ix \cdot \xi}}{|\xi|^2 + 2k(\xi_1 + i\xi_2)} d\xi,$$

as well as the associated single layer potential

$$(S_k \phi)(x) := \int_{\partial\mathbb{D}} G_k(x - y) \phi(y) d\sigma(y),$$

play a crucial role. Here $k \in \mathbb{C}$ and $x \in \mathbb{R}^2$ and $kx = (k_1 + ik_2)(x_1 + ix_2)$. The reconstruction method of Nachman [71] from infinite-precision data consists of the following two steps:

Step 1: From boundary measurements Λ_γ to scattering transform \mathbf{t} . For each fixed $k \in \mathbb{C}$, solve in $H^{1/2}(\partial\mathbb{D})$ the integral equation

$$(1.3) \quad \psi(\cdot, k)|_{\partial\mathbb{D}} = e^{ikx} - S_k(\Lambda_\gamma - \Lambda_1)\psi(\cdot, k)|_{\partial\mathbb{D}},$$

where the DN map of the homogeneous conductivity 1 is denoted by Λ_1 . Then substitute ψ in the formula for the scattering transform $\mathbf{t} : \mathbb{C} \rightarrow \mathbb{C}$:

$$(1.4) \quad \mathbf{t}(k) = \int_{\partial\mathbb{D}} e^{i\bar{k}\bar{x}} (\Lambda_\gamma - \Lambda_1)\psi(\cdot, k) d\sigma,$$

where $d\sigma$ denotes arclength measure on $\partial\mathbb{D}$.

Step 2: From scattering transform \mathbf{t} to conductivity γ . Denote $e_x(k) := \exp(i(kx + \bar{k}\bar{x}))$. For each fixed $x \in \mathbb{D}$, solve the integral equation

$$(1.5) \quad \mu(x, k) = 1 + \frac{1}{(2\pi)^2} \int_{\mathbb{R}^2} \frac{\mathbf{t}(k')}{(k - k')k'} e_{-x}(k') \overline{\mu(x, k')} dk'_1 dk'_2;$$

then $\gamma(x) = \mu(x, 0)^2$.

The integral equation (1.5) was obtained from a corresponding differential equation, a so-called D-bar equation, which involves the derivative with respect to the complex variable \bar{k} . This is where the D-bar method gets its name.

The above Steps 1 and 2 are not directly applicable to practical measurement data $\Lambda_\gamma^\varepsilon$. A numerical EIT algorithm starting from $\Lambda_\gamma^\varepsilon$ has been implemented with Step 1 linearized using Born approximation and Step 2 simplified by truncating \mathbf{t} . That algorithm has been applied to simulated data in [53, 67, 68, 82, 83] and to laboratory and *in vivo* human data in [41, 42, 69], resulting in useful reconstructions of both smooth and piecewise smooth conductivities. Further, a reconstruction method based on [14] is given in [50, 51, 56] and a 3-D algorithm for small conductivities is outlined, but not implemented in [19]. A direct reconstruction algorithm for 3-D based on [70] was implemented in [8]. At this time there is no regularization analysis available for the above algorithms.

In this work we present modified Steps 1 and 2 applicable to practical measurements and demonstrate the method with simulated data. Further, we formulate the method in a way that allows an asymptotic regularization analysis.

The *forward map* $F : \gamma \mapsto \Lambda_\gamma$ takes a conductivity to the corresponding boundary measurement. We consider F acting between the spaces

$$F : \mathcal{D}(F) \subset L^\infty(\mathbb{D}) \rightarrow Y$$

defined as follows.

Definition 1.1. *Let $M > 0$ and $0 < \rho < 1$ and take the domain $\mathcal{D}(F)$ to be the set of functions $\gamma : \mathbb{D} \rightarrow \mathbb{R}$ satisfying*

$$(1.6) \quad \|\gamma\|_{C^2(\bar{\mathbb{D}})} \leq M,$$

$$(1.7) \quad \gamma(x) \geq M^{-1} \quad \text{for every } x \in \mathbb{D},$$

$$(1.8) \quad \gamma(x) \equiv 1 \quad \text{for } \rho < |x| < 1.$$

The set $\mathcal{D}(F)$ inherits a metric space structure from $L^\infty(\mathbb{D})$.

The data space $Y \subset \mathcal{L}(H^{1/2}(\partial\mathbb{D}), H^{-1/2}(\partial\mathbb{D}))$ consists of bounded linear operators $A : H^{1/2}(\partial\mathbb{D}) \rightarrow H^{-1/2}(\partial\mathbb{D})$ satisfying

$$(1.9) \quad A(1) = 0,$$

$$(1.10) \quad \int_{\partial\mathbb{D}} A(f) d\sigma = 0 \quad \text{for every } f \in H^{1/2}(\partial\mathbb{D}).$$

We equip Y with the usual operator norm $\|\cdot\|_Y = \|\cdot\|_{H^{1/2}(\partial\mathbb{D}) \rightarrow H^{-1/2}(\partial\mathbb{D})}$.

The constants M and ρ are *a priori* knowledge about the unknown conductivity.

We denote $\mathcal{E} := \Lambda_\gamma^\varepsilon - \Lambda_\gamma$ and assume that

$$(1.11) \quad \mathcal{E} \in Y, \quad \|\mathcal{E}\|_Y \leq \varepsilon,$$

where $\varepsilon > 0$ denotes the (known) noise level. The one-dimensional conditions (1.9) and (1.10) can usually be easily enforced, see Section 4.3 below. We remark that in some applications \mathcal{E} may not naturally belong to Y ; in that case an extra step of projecting $\Lambda_\gamma^\varepsilon$ to Y might be needed. We do not discuss such procedures further.

We adapt Definitions 3.1 of [22] and 2.1 and 2.3 of [49] to the present nonlinear setting in Banach spaces as follows:

Definition 1.2. A family of continuous mappings $\Gamma_\alpha : Y \rightarrow L^\infty(\mathbb{D})$ parameterized by $0 < \alpha < \infty$ is a regularization strategy for F if

$$(1.12) \quad \lim_{\alpha \rightarrow 0} \|\Gamma_\alpha \Lambda_\gamma - \gamma\|_{L^\infty(\mathbb{D})} = 0$$

for each fixed $\gamma \in \mathcal{D}(F)$. Further, a regularization strategy with a choice $\alpha = \alpha(\varepsilon)$ of regularization parameter as function of noise level is called admissible if

$$(1.13) \quad \alpha(\varepsilon) \rightarrow 0 \text{ as } \varepsilon \rightarrow 0,$$

and for any fixed $\gamma \in \mathcal{D}(F)$ the following holds:

$$(1.14) \quad \sup_{\Lambda_\gamma^\varepsilon} \{\|\Gamma_{\alpha(\varepsilon)} \Lambda_\gamma^\varepsilon - \gamma\|_{L^\infty(\mathbb{D})} : \|\Lambda_\gamma^\varepsilon - \Lambda_\gamma\|_Y \leq \varepsilon\} \rightarrow 0 \text{ as } \varepsilon \rightarrow 0.$$

This is an outline of the regularized D-bar method we propose:

Step 1 $^\varepsilon$: From noisy data $\Lambda_\gamma^\varepsilon$ to regularized scattering transform \mathbf{t}_R^ε . Given the noise level $\varepsilon > 0$, solve equation

$$(1.15) \quad \psi^\varepsilon(\cdot, k)|_{\partial\mathbb{D}} = e^{ikx} - S_k(\Lambda_\gamma^\varepsilon - \Lambda_1)\psi^\varepsilon(\cdot, k)|_{\partial\mathbb{D}}$$

for $|k| < R(\varepsilon) = -\frac{1}{10} \log \varepsilon$. Substitute the solution ψ^ε into the formula for the truncated scattering transform $\mathbf{t}_R^\varepsilon : \mathbb{C} \rightarrow \mathbb{C}$:

$$(1.16) \quad \mathbf{t}_R^\varepsilon(k) = \begin{cases} \int_{\partial\mathbb{D}} e^{i\bar{k}\bar{x}} (\Lambda_\gamma^\varepsilon - \Lambda_1)\psi^\varepsilon(\cdot, k) d\sigma & \text{for } |k| < R(\varepsilon), \\ 0, & \text{otherwise.} \end{cases}$$

Step 2 $^\varepsilon$: From \mathbf{t}_R^ε to reconstruction $\Gamma_\alpha \Lambda_\gamma^\varepsilon$. For each fixed $x \in \mathbb{D}$, solve

$$(1.17) \quad \mu_R^\varepsilon(x, k) = 1 + \frac{1}{(2\pi)^2} \int_{|k'| < R} \frac{\mathbf{t}_R^\varepsilon(k')}{(k - k')k'} e^{-x(k')} \overline{\mu_R^\varepsilon(x, k')} dk'_1 dk'_2,$$

and define

$$(1.18) \quad (\Gamma_{\alpha(\varepsilon)} \Lambda_\gamma^\varepsilon)(x) := (\mu_R^\varepsilon(x, 0))^2$$

with $\alpha(\varepsilon) = 1/R(\varepsilon)$.

We prove in Theorems 3.1 and 3.2 below that Steps 1 $^\varepsilon$ and Step 2 $^\varepsilon$ (combined with a spectral extension detailed in Section 3) define a regularization strategy with admissible parameter choice in the sense of Definition 1.2. Moreover, we give an explicit decay estimate for the convergence in (1.14). The proofs involve careful discussion of the solvability of equation (1.15) and the domain and continuity of the map Γ_α . Furthermore, we illustrate the method by numerical simulations.

Let us review the history of CGO-based results on the inverse conductivity problem. Calderón solved in [17] a linearized version of the question. Unique determination of an infinitely smooth isotropic conductivity from the DN map in dimension $n \geq 3$ was shown in [87]. This result has been extended to conductivities having $\frac{3}{2}$ derivatives in [13, 75], and in [29] for conductivities having $C^{1,\alpha}$ -smooth conormal singularities on submanifolds. In dimension two, unique identifiability of isotropic conductivities was proven in [71] for twice differentiable conductivities. Reduction to one derivative was provided in [14], and Calderón's original L^∞ question was answered in [1]. For dimension $n \geq 3$ constructive reconstruction algorithms were proposed in [70, 74]. For the case of anisotropic conductivities, see [2, 71, 85, 86]. Other CGO-based algorithms have been developed for detection of inclusions, for example see [15, 37, 38, 88]. For recent development on new kinds of CGO solutions for inverse problems, see [16, 20, 47, 55].

Finally, we note that relaxing the boundedness and strict positivity assumptions on the conductivity leads to interesting results on uniqueness and non-uniqueness. Counterexamples can be found when the conductivity is allowed to be only positive semi-definite [30, 31, 61]. These examples bridge Calderón's inverse problem, invisibility cloaking, and transformation optics [27, 28, 32]. The limit of degeneracy of conductivity problem for which the inverse problems is uniquely solvable is studied in [3].

Classical regularization theory is explained in [22, 49]. Iterative regularization of both linear and nonlinear inverse problems and convergence rates are discussed in Hilbert space setting in [9, 33, 35, 65, 66] and in Banach space setting in [34, 44, 45, 48, 76, 77, 78]. Regularized iterative solution methods for electrical impedance tomography are analyzed in [63, 79]. Non-iterative regularized inversion for blind deconvolution is presented in [43], and for the restricted problem of finding inclusions in conductivity from EIT data in [62] based on the asymptotic analysis in [36]. Our new results, based on the use of CGO solutions, provide an example of a non-iterative regularization method (with an explicit, but not necessarily optimal, convergence rate in Banach spaces) for the nonlinear inverse conductivity problem.

Note that our new results provide an *unconditional* stability analysis for the inverse conductivity problem. Conditional stability analyses for D-bar methods, such as [4, 5, 64], are typically of the form

$$(1.19) \quad \|\gamma_1 - \gamma_2\|_Z \leq f(\|\Lambda_{\gamma_1} - \Lambda_{\gamma_2}\|_Y),$$

where γ_1, γ_2 belong to some appropriate function space Z and f is a continuous function with $f(0) = 0$. While theoretically valuable, inequalities of the form (1.19) are not enough to analyze instability caused by practical measurement errors. Namely, there is no guarantee that the measured noisy operator $\Lambda_\gamma^\varepsilon$ would be the DN map corresponding to any conductivity. In contrast, we prove the estimate

$$\|\Gamma_{\alpha(\varepsilon)}\Lambda_\gamma^\varepsilon - \gamma\|_{L^\infty(\mathbb{D})} \leq C(-\log \varepsilon)^{-1/14},$$

where $\|\Lambda_\gamma^\varepsilon - \Lambda_\gamma\|_Y \leq \varepsilon$ and ε is small.

This paper is organized as follows. Section 2 contains the the main technical results. It is shown that from noisy data an approximation of the scattering transform can be computed, and furthermore an estimate of the error is obtained. Next in Section 3 we give the definition of the regularized reconstruction method and show that the method is in fact a regularization method in the sense of Definition 1.2. Then in Section 4 we give the numerical implementation of the regularized reconstruction method, and finally in Section 5 we show numerical results.

We denote the set of bounded linear operators $A : X_1 \rightarrow X_2$ between Banach spaces X_1 and X_2 by $\mathcal{L}(X_1, X_2)$ and use the abbreviation $\mathcal{L}(X_1) := \mathcal{L}(X_1, X_1)$. We denote the operator norm of $A : H^{1/2}(\partial\mathbb{D}) \rightarrow H^{1/2}(\partial\mathbb{D})$ by $\|A\|_{1/2}$. The notation C is reserved for generic constants that may change from line to line. In contrast, C_1, C_2, \dots are constants with specific values.

2. TECHNICAL ESTIMATES

The continuous dependence of the solution to the D-bar equation on the scattering transform was considered in several papers [4, 53, 64, 67]. We will simplify the general result from [53] in a way suitable for the context here:

Lemma 2.1. *Let $4/3 < r_0 < 2$ and suppose that $\phi_1, \phi_2 \in L^r(\mathbb{R}^2)$ for all $r \geq r_0$. Let μ_1, μ_2 , be the solutions of*

$$\mu_j(x, k) = 1 + \frac{1}{(2\pi)^2} \int_{\mathbb{R}^2} \frac{\phi_j(k')}{(k - k')} \overline{\mu_j(x, k')} dk'_1 dk'_2, \quad j = 1, 2.$$

Then for fixed $x \in \overline{\mathbb{D}}$ we have

$$(2.1) \quad \|\mu_1(x, \cdot) - \mu_2(x, \cdot)\|_{C^\alpha(\mathbb{R}^2)} \leq C \|\phi_1 - \phi_2\|_{L^{r_0} \cap L^{r_0'}(\mathbb{R}^2)},$$

where $\alpha < 2/r_0 - 1$ and $1/r_0' = 1 - 1/r_0$. The constant C in (2.1) is independent of x and depends on $\sup_{p \in [r_0, r_0'], j=1,2} \|\phi_j\|_{L^p(\mathbb{R}^2)}$.

Proof. The function $\mu_1 - \mu_2$ satisfies the integral equation

$$(2.2) \quad \begin{aligned} (\mu_1 - \mu_2)(x, k) &= \frac{1}{\pi} \int_{\mathbb{R}^2} \frac{\phi_2(x, k')}{k - k'} \overline{(\mu_1 - \mu_2)(x, k')} dk'_1 dk'_2 \\ &+ \frac{1}{\pi} \int_{\mathbb{R}^2} \frac{(\phi_1 - \phi_2)(x, k')}{k - k'} \overline{(\mu_1(x, k))} dk'_1 dk'_2 \end{aligned}$$

or equivalently the D-bar equation

$$\bar{\partial}_k(\mu_1 - \mu_2) = \phi_2 \overline{(\mu_1 - \mu_2)} + (\phi_1 - \phi_2) \overline{\mu_1}.$$

As a consequence of [4, Lemma 2.6] we have for $1/\tilde{r}_0 = 1/r_0 - 1/2$ that

$$(2.3) \quad \begin{aligned} \|\mu_1 - \mu_2\|_{L^{\tilde{r}_0}(\mathbb{R}^2)} &\leq C \|(\phi_1 - \phi_2) \overline{\mu_1}\|_{L^{r_0}(\mathbb{R}^2)} \\ &\leq C \|\phi_1 - \phi_2\|_{L^{r_0}(\mathbb{R}^2)} \|\mu_1\|_{L^\infty(\mathbb{R}^2)} \\ &\leq C \|\phi_1 - \phi_2\|_{L^{r_0}(\mathbb{R}^2)}, \end{aligned}$$

where C depends on $\|\phi_j\|_{L^p(\mathbb{R}^2)}$, $j = 1, 2$, for several $p \geq r_0$.

The integral operator appearing in (2.2) is the solid Cauchy transform

$$Pf(z) = -\frac{1}{\pi} \int_{\mathbb{C}} \frac{f(\lambda)}{\lambda - z} dm(\lambda),$$

where dm denotes Lebesgue measure on \mathbb{C} . Combining the mapping properties of P , see [89, Theorem 1.21], with estimate (2.3) yields

$$\begin{aligned} &\|\mu_1 - \mu_2\|_{C^\alpha(\mathbb{R}^2)} \\ &\leq C (\|\phi_2 \overline{(\mu_1 - \mu_2)}\|_{L^{r_0} \cap L^{r_0'}(\mathbb{R}^2)} + \|(\phi_1 - \phi_2) \overline{\mu_1}\|_{L^{r_0} \cap L^{r_0'}(\mathbb{R}^2)}) \\ &\leq C (\|\phi_2\|_{L^2 \cap L^s(\mathbb{R}^2)} \|\mu_1 - \mu_2\|_{L^{\tilde{r}_0}(\mathbb{R}^2)} + \|\phi_1 - \phi_2\|_{L^{r_0} \cap L^{r_0'}(\mathbb{R}^2)} \|\mu_1\|_{L^\infty(\mathbb{R}^2)}) \\ &\leq C \|\phi_1 - \phi_2\|_{L^{r_0} \cap L^{r_0'}(\mathbb{R}^2)} \end{aligned}$$

where $1/s = 3/2 - 2/r_0$ (which implies $2 < s < \infty$). \square

Recall that the convolution operator with kernel g_k defined in (1.2) is bounded between various Sobolev spaces. Indeed we have the estimate

$$(2.4) \quad \|g_k * v\|_{H^s(\mathbb{D})} \leq C |k|^{s-1} \|v\|_{L^2(\mathbb{D})}, \quad 0 \leq s \leq 2,$$

uniformly for $k \geq K_0$ for any $K_0 > 0$. For $s = 0$ the result was obtained in [87]. The generalization seems to be well established in the literature [11, 80].

We need a lemma concerning the mapping properties of S_k . We know from [71, Lemma 7.1] that $S_k: H^{-1/2}(\partial\mathbb{D}) \rightarrow H^{1/2}(\partial\mathbb{D})$ is a bounded linear operator. We will need a bound on the operator norm. Denote the standard Green's function for the Laplace operator by $G_0(x) = -(2\pi)^{-1} \log|x|$ and set $H_k(x) = G_k(x) - G_0(x)$.

The function H_k is harmonic: $\Delta H_k = \Delta(G_k - G_0) = \delta - \delta = 0$, and consequently $H_k \in C^\infty(\mathbb{R}^2)$. Use the identity $g_k(x) = g_1(kx)$ to compute

$$(2.5) \quad H_k(x) = e^{ikx} g_k(x) + \frac{1}{2\pi} \log|x| = e^{ikx} g_1(kx) + \frac{1}{2\pi} \log|kx| - \frac{1}{2\pi} \log|k|.$$

The above shows that

$$(2.6) \quad H_k(x) = H_1(kx) - \frac{1}{2\pi} \log|k|.$$

Furthermore, denote $\tilde{H}_1(x) := H_1(x) - H_1(0)$; then $\tilde{H}_1(0) = 0$. Use the above to decompose the single layer operator S_k as

$$(2.7) \quad \begin{aligned} S_k \phi(x) &= \int_{\partial\mathbb{D}} G_k(x-y) \phi(y) d\sigma(y) \\ &= \int_{\partial\mathbb{D}} G_0(x-y) \phi(y) d\sigma(y) + \int_{\partial\mathbb{D}} H_k(x-y) \phi(y) d\sigma(y) \\ &= S_0 \phi(x) + \mathcal{H}_k \phi(x) - \left(H_1(0) + \frac{\log|k|}{2\pi} \right) \int_{\partial\mathbb{D}} \phi(y) d\sigma(y), \end{aligned}$$

where the integral operator \mathcal{H}_k is defined by

$$(2.8) \quad \mathcal{H}_k \phi(x) = \int_{\partial\mathbb{D}} \tilde{H}_1(k(x-y)) \phi(y) d\sigma(y).$$

We can now prove the lemma.

Lemma 2.2. *Let $\phi_0 \in H^{-1/2}(\partial\mathbb{D})$ with $\int_{\partial\mathbb{D}} \phi_0(y) d\sigma(y) = 0$. Then*

$$(2.9) \quad \|S_k \phi_0\|_{H^{1/2}(\partial\mathbb{D})} \leq C_1 e^{2|k|} (1 + |k|) \|\phi_0\|_{H^{-1/2}(\partial\mathbb{D})},$$

where the constant C_1 is independent of k .

Proof. First we consider $k \in \mathbb{C}$ with $|k| \leq 1$. Then $S_k \phi_0 = S_0 \phi_0 + \mathcal{H}_k \phi_0$. By extending the definition of $\mathcal{H}_k \phi_0$ by allowing any $x \in \mathbb{D}$ in (2.8) we can estimate by Minkowski's inequality and change of variables

$$(2.10) \quad \begin{aligned} \|\mathcal{H}_k \phi_0\|_{H^{1/2}(\partial\mathbb{D})} &\leq \|\mathcal{H}_k \phi_0\|_{H^1(\mathbb{D})} \\ &\leq C \left(\int_{\mathbb{D}} \int_{\partial\mathbb{D}} |\tilde{H}_1(k(x-y)) \phi_0(y)| d\sigma(y)^2 dx^{1/2} \right. \\ &\quad \left. + \int_{\mathbb{D}} \int_{\partial\mathbb{D}} |\nabla(\tilde{H}_1(k(x-y))) \phi_0(y)| d\sigma(y)^2 dx^{1/2} \right) \\ &\leq \|\tilde{H}_1(k(x-y))\|_{H^1(\mathbb{D})} \int_{\partial\mathbb{D}} |\phi_0(y)| d\sigma(y) \\ &\leq C \left(|k|^{1/2} \max_{\mathbb{D}} |\tilde{H}_1(\frac{k}{|k|}x)| + |k|^{3/2} \max_{\mathbb{D}} |\nabla \tilde{H}_1(\frac{k}{|k|}x)| \right) \|\phi_0\|_{H^{-1/2}(\partial\mathbb{D})} \\ &\leq C |k|^{1/2} \|\phi_0\|_{H^{-1/2}(\partial\mathbb{D})}, \end{aligned}$$

from which (2.9) follows by the smoothness of \tilde{H}_1 .

Now consider $|k| > 1$. We then have for $x \in \mathbb{R}^2 \setminus \overline{\mathbb{D}}$ by using integration by parts that

$$S_k \phi_0(x) = \langle G_k(x - \cdot), \phi_0 \rangle = \int_{\mathbb{D}} \nabla_y G_k(x-y) \cdot \nabla u(y) dy = -\nabla_x (G_k * (\nabla u)),$$

where $\Delta u = 0$ in \mathbb{D} and $\partial_\nu u = \phi_0$ on $\partial\mathbb{D}$. By continuity the formula remains valid also for $x \in \partial\mathbb{D}$. We then find

$$\begin{aligned} \|S_k \phi_0\|_{H^{1/2}(\partial\mathbb{D})} &\leq \|\nabla(G_k * (\nabla u))\|_{H^1(\mathbb{D})} \\ &\leq \|G_k * (\nabla u)\|_{H^2(\mathbb{D})} \\ &\leq \|e^{ixk} g_k * (e^{-iyk} \nabla u)\|_{H^2(\mathbb{D})} \\ &\leq C e^{|k|} (|k| + 1) \|e^{-iyk} \nabla u\|_{L^2(\mathbb{D})} \\ &\leq C e^{|k|} (|k| + 1) \|\nabla u\|_{L^2(\mathbb{D})} \\ &\leq C e^{|k|} (|k| + 1) \|\phi_0\|_{H^{-1/2}(\partial\mathbb{D})}, \end{aligned}$$

where in the fourth inequality we have used (2.4) and Leibniz' rule. \square

Define a linear operator $B_k \in \mathcal{L}(H^{1/2}(\partial\mathbb{D}))$ by the formula

$$(2.11) \quad B_k := I + S_k(\Lambda_\gamma - \Lambda_1).$$

Note that the solution of the boundary integral equation (1.3) can be written as $B_k^{-1}(e^{ikx}|_{\partial\mathbb{D}})$. Next we will find a bound on the norm of B_k^{-1} :

Lemma 2.3. *For $k \in \mathbb{C}$ we have the estimate*

$$(2.12) \quad \|B_k^{-1}\|_{1/2} = \|(I + S_k(\Lambda_\gamma - \Lambda_1))^{-1}\|_{1/2} \leq C_2 e^{2|k|} (1 + |k|),$$

where the constant C_2 is independent of k and depends only on the a priori knowledge M and ρ .

Proof. We first prove (2.12) for small $|k|$. Let S_0 be defined by (2.7) and set $B_0 := I + S_0(\Lambda_\gamma - \Lambda_1)$. The operator B_0 is known to be invertible in $\mathcal{L}(H^{1/2}(\partial\mathbb{D}))$ by [19, Lemma 3.3]. By Green's formula

$$\int_{\partial\mathbb{D}} \Lambda_\gamma f d\sigma = 0 = \int_{\partial\mathbb{D}} \Lambda_1 f d\sigma$$

for all $f \in H^{1/2}(\partial\mathbb{D})$, so we may use (2.7) to write

$$B_k - B_0 = \mathcal{H}_k(\Lambda_\gamma - \Lambda_1).$$

Recall the definition (2.8) of the integral operator \mathcal{H}_k . Now \tilde{H}_1 is an infinitely smooth function satisfying $\tilde{H}_1(0) = 0$, so $\|\mathcal{H}_k(\Lambda_\gamma - \Lambda_1)\|_{1/2} \rightarrow 0$ as $|k| \rightarrow 0$. Thus there exists some $k_0 > 0$ for which it holds that

$$\|\mathcal{H}_k(\Lambda_\gamma - \Lambda_1)\|_{1/2} < \frac{1}{2\|B_0^{-1}\|_{1/2}} \quad \text{whenever } |k| \leq k_0,$$

so we may conclude that for all $|k| \leq k_0$

$$\|B_k^{-1}\|_{1/2} \leq \|B_0^{-1}\|_{1/2} \|(I + B_0^{-1}\mathcal{H}_k(\Lambda_\gamma - \Lambda_1))^{-1}\|_{1/2} \leq 2\|B_0^{-1}\|_{1/2}.$$

The estimate (2.12) thus follows for $|k| \leq k_0$.

Next consider $|k| > k_0$. Let $f \in H^{1/2}(\partial\mathbb{D})$ and define

$$h = [I + S_k(\Lambda_\gamma - \Lambda_1)]f.$$

In \mathbb{D} define v_f to be the solution to $(\Delta + q)v_f = 0$ in \mathbb{D} with $v_f|_{\partial\mathbb{D}} = f$ and $q = \gamma^{-1/2}\Delta\gamma^{1/2}$. Define $v := v_f + u^{\text{exp}}$ and $u^{\text{exp}} := G_k * (qv_f)$ and note that v solves the Dirichlet problem

$$\Delta v = 0 \text{ in } \mathbb{D}, \quad v|_{\partial\mathbb{D}} = h.$$

We can then estimate

$$\begin{aligned}
\|f\|_{H^{1/2}(\partial\mathbb{D})} &\leq \|v_f\|_{H^1(\mathbb{D})} \\
&= \|v - G_k * (qv_f)\|_{H^1(\mathbb{D})} \\
&\leq \|v\|_{H^1(\mathbb{D})} + \|u^{\text{exp}}\|_{H^1(\mathbb{D})} \\
(2.13) \qquad &\leq \|h\|_{H^{1/2}(\partial\mathbb{D})} + \|u^{\text{exp}}\|_{H^1(\mathbb{D})}.
\end{aligned}$$

In order to estimate u^{exp} we note that

$$\Delta u^{\text{exp}} = qv_f = q(v - u^{\text{exp}}).$$

Conjugating with exponentials yields

$$(\Delta + 4k\partial + q)u = e^{-ikx}qv, \quad u := e^{-ikx}u^{\text{exp}} = g_k * (e^{-ikx}qv_f),$$

which implies

$$u = (I + g_k * (q))^{-1}(g_k * (e^{-ikx}qv)).$$

Since the operator g_k* is uniformly bounded from $L^2(\mathbb{D})$ into $H^1(\mathbb{D})$ for $k > k_0$ (see (2.4)) we then obtain

$$\begin{aligned}
\|u^{\text{exp}}\|_{H^1(\mathbb{D})} &= \|e^{ikx}u\|_{H^1(\mathbb{D})} \\
&\leq \|e^{ikx}\|_{W^{1,\infty}(\mathbb{D})} \|u\|_{H^1(\mathbb{D})} \\
&\leq Ce^{|k|}(1 + |k|) \|g_k * (e^{-ikx}qv)\|_{H^1(\mathbb{D})} \\
&\leq Ce^{|k|}(1 + |k|) \|e^{-ikx}qv\|_{L^2(\mathbb{D})} \\
&\leq Ce^{2|k|}(1 + |k|) \|q\|_{L^\infty(\mathbb{D})} \|v\|_{H^1(\mathbb{D})} \\
&\leq Ce^{2|k|}(1 + |k|) \|h\|_{H^{1/2}(\partial\mathbb{D})},
\end{aligned}$$

which together with (2.13) proves the claim. \square

The following result gives information about solvability of the noisy boundary integral equation (1.15) and about how \mathbf{t}_R^ε defined in (1.16) of Step 1^ε approximates \mathbf{t} defined in (1.4) of Step 1.

Lemma 2.4. *There exists a positive constant $\varepsilon_0 > 0$, depending only on M and ρ , with the following properties. Equation (1.15) is solvable in $H^{1/2}(\partial\mathbb{D})$ for all $0 < \varepsilon < \varepsilon_0$ and $|k| < R$ with*

$$(2.14) \qquad R = R(\varepsilon) = -\frac{1}{10} \log \varepsilon.$$

Furthermore, for all $0 < \varepsilon < \varepsilon_0$ and any $p > 1$ we have the estimate

$$(2.15) \qquad \left\| \frac{\mathbf{t}(k) - \mathbf{t}_R^\varepsilon(k)}{k} \right\|_{L^p(|k| \leq R(\varepsilon))} \leq C \left(-\frac{1}{10} \log \varepsilon \right)^{2/p} \varepsilon^{1/10},$$

where C is independent of p and R and ε .

Note that the right hand side of (2.15) tends to zero as $\varepsilon \rightarrow 0$.

Proof. Define a linear operator $B_k^\varepsilon \in \mathcal{L}(H^{1/2}(\partial\mathbb{D}))$ by the formula

$$(2.16) \qquad B_k^\varepsilon := I + S_k(\Lambda_\gamma^\varepsilon - \Lambda_1).$$

Compare (2.16) to (2.11) and note that the assumption that $\gamma(x) \equiv 1$ in a neighborhood of $\partial\mathbb{D}$ implies that $S_k(\Lambda_\gamma - \Lambda_1)$ is a compact operator on $H^{1/2}(\partial\mathbb{D})$, so

B_k is a Fredholm operator of the form “identity+compact”, but the operator B_k^ε cannot be expected in general to be of that form.

The solution of the boundary integral equation (1.15) can now be written as $(B_k^\varepsilon)^{-1}(e^{ikx}|_{\partial\mathbb{D}})$. Define $A_k^\varepsilon := S_k \mathcal{E} B_k^{-1}$ and note that $B_k^\varepsilon = [I + A_k^\varepsilon] B_k$. Let $|k| \leq R$. Since \mathcal{E} maps onto functions on the boundary with mean zero by (1.11), we can apply Lemma 2.2 and Lemma 2.3 to obtain

$$\|A_k^\varepsilon\|_{1/2} = \|S_k \mathcal{E} B_k^{-1}\|_{1/2} \leq C_1 C_2 \varepsilon e^{4R} (1+R)^2.$$

Substituting (2.14) gives

$$\|A_k^\varepsilon\|_{1/2} \leq C_1 C_2 \varepsilon^{6/10} (1 - \frac{1}{10} (\log \varepsilon))^2,$$

and thus we see that there exists $0 < \varepsilon_0 < 1$ for which $\|A_k^\varepsilon\|_{1/2} < \frac{1}{2}$ whenever $0 < \varepsilon < \varepsilon_0$. For those ε the operator $I + A_k^\varepsilon$ is invertible with $\|[I + A_k^\varepsilon]^{-1}\|_{1/2} < 2$ and we may write

$$(2.17) \quad (B_k^\varepsilon)^{-1} = B_k^{-1} [I + A_k^\varepsilon]^{-1}.$$

Note that $\psi^\varepsilon = (B_k^\varepsilon)^{-1}(e^{ikx}|_{\partial\mathbb{D}})$ and $\psi = B_k^{-1}(e^{ikx}|_{\partial\mathbb{D}})$. We can estimate for $0 < \varepsilon < \varepsilon_0$ using Lemma 2.3

$$\begin{aligned} \|\psi^\varepsilon(x, k)\|_{H^{1/2}(\partial\mathbb{D})} &\leq \|(B_k^\varepsilon)^{-1}\|_{1/2} \|e^{ikx}\|_{H^{1/2}(\partial\mathbb{D})} \\ &\leq 2 \|B_k^{-1}\|_{1/2} \|e^{ikx}\|_{H^{1/2}(\partial\mathbb{D})} \\ &\leq C e^{3|k|} (1 + |k|)^2 \\ &\leq C e^{4R} \\ (2.18) \quad &= C \varepsilon^{-4/10} \end{aligned}$$

by the choice (2.14) of $R(\varepsilon)$. Further, by Lemma 2.3 and (2.17) and using Neumann series we can estimate

$$\begin{aligned} \|(B_k^\varepsilon)^{-1} - B_k^{-1}\|_{1/2} &\leq \|B_k^{-1}\|_{1/2} \|[I + A_k^\varepsilon]^{-1} - I\|_{1/2} \\ &\leq \|B_k^{-1}\|_{1/2} \|A_k^\varepsilon\|_{1/2} \|[I + A_k^\varepsilon]^{-1}\|_{1/2} \\ &\leq 2C_1 C_2^2 e^{6R} (1+R)^3 \varepsilon \\ &\leq C e^{7R} \varepsilon \end{aligned}$$

for $0 < \varepsilon < \varepsilon_0$. Then

$$\begin{aligned} \|\psi^\varepsilon(\cdot, k) - \psi(\cdot, k)\|_{H^{1/2}(\partial\mathbb{D})} &= \|((B_k^\varepsilon)^{-1} - B_k^{-1})e^{ikx}\|_{H^{1/2}(\partial\mathbb{D})} \\ &\leq \|(B_k^\varepsilon)^{-1} - B_k^{-1}\|_{1/2} \|e^{ikx}\|_{H^{1/2}(\partial\mathbb{D})} \\ &\leq 2C_1 C_2^2 e^{7R} (1+R)^4 \varepsilon \\ &\leq C e^{8R(\varepsilon)} \varepsilon \\ (2.19) \quad &\leq C \varepsilon^{2/10}. \end{aligned}$$

Combining (1.11), (2.18) and (2.19) shows for $0 < \varepsilon < \varepsilon_0$ and $|k| < R(\varepsilon)$ that

$$\begin{aligned}
& \left| \frac{\mathbf{t}(k) - \mathbf{t}_R^\varepsilon(k)}{\bar{k}} \right| \\
&= \left| \int_{\partial\mathbb{D}} \frac{e^{i\bar{k}\bar{x}}}{\bar{k}} ((\Lambda_\gamma - \Lambda_1)\psi(\cdot, k) - (\Lambda_\gamma^\varepsilon - \Lambda_1)\psi^\varepsilon(\cdot, k)) d\sigma(x) \right| \\
&= \left| \int_{\partial\mathbb{D}} \frac{(e^{i\bar{k}\bar{x}} - 1)}{\bar{k}} ((\Lambda_\gamma - \Lambda_1)\psi(\cdot, k) - (\Lambda_\gamma^\varepsilon - \Lambda_1)\psi^\varepsilon(\cdot, k)) d\sigma(x) \right| \\
&\leq \left\| \frac{e^{i\bar{k}\bar{x}} - 1}{\bar{k}} \right\|_{H^{1/2}(\partial\mathbb{D})} (\|\Lambda_\gamma - \Lambda_1\|_Y \|\psi^\varepsilon(\cdot, k) - \psi(\cdot, k)\|_{H^{1/2}(\partial\mathbb{D})} + \varepsilon \|\psi^\varepsilon(\cdot, k)\|_{H^{1/2}(\partial\mathbb{D})}) \\
&\leq Ce^R (\varepsilon^{2/10} + \varepsilon^{6/10}) \\
&\leq C\varepsilon^{1/10}.
\end{aligned}$$

Above we used the fact that $\|\Lambda_\gamma - \Lambda_1\|_Y \leq C$ for some constant depending only on the *a priori* constant M (this can be seen using triangle inequality, basic elliptic estimates and the Sobolev trace theorem). For any $p > 1$ and $0 < \varepsilon < \varepsilon_0$ we then get

$$\begin{aligned}
\left\| \frac{\mathbf{t}(k) - \mathbf{t}_R^\varepsilon(k)}{\bar{k}} \right\|_{L^p(|k| \leq R(\varepsilon))}^p &\leq C\varepsilon^{p/10} \int_{|k| \leq R(\varepsilon)} 1 dk_1 dk_2 \\
&\leq C\varepsilon^{p/10} R(\varepsilon)^2 \\
&\leq C\varepsilon^{p/10} \left(-\frac{1}{10} \log \varepsilon\right)^2,
\end{aligned}$$

which gives (2.15). \square

3. REGULARIZED D-BAR METHOD

Recall the map Γ_α defined by Steps 1 $^\varepsilon$ and 2 $^\varepsilon$ in the Introduction. We first show that Γ_α is well-defined on a subset of Y and has desirable convergence properties.

Theorem 3.1. *Let \mathbb{D} be the unit disk. Assume $M > 0$ and $0 < \rho < 1$ are given, and let $\mathcal{D}(F)$ be as in Definition 1.1. Then there exists a constant $\varepsilon_0 > 0$, depending only on M and ρ , with the following properties. Let $\gamma \in \mathcal{D}(F)$ be arbitrary and let $\Lambda_\gamma^\varepsilon = \Lambda_\gamma + \mathcal{E}$ with $\|\mathcal{E}\|_Y \leq \varepsilon < \varepsilon_0$. Then $\Gamma_{\alpha(\varepsilon)}\Lambda_\gamma^\varepsilon$ is well-defined by (1.18) and satisfies the estimate*

$$(3.1) \quad \|\Gamma_{\alpha(\varepsilon)}\Lambda_\gamma^\varepsilon - \gamma\|_{L^\infty(\mathbb{D})} \leq C(-\log \varepsilon)^{-1/14}.$$

Proof. Let ε_0 be as in Lemma 2.4, suppose $0 < \varepsilon < \varepsilon_0$ and set $R(\varepsilon) = -\frac{1}{10} \log(\varepsilon)$. Note that ε_0 is by construction so small that $R(\varepsilon) > 0$. Then by Lemma 2.4 the equation (1.15) has a unique solution ψ^ε . We substitute ψ^ε to the formula (1.16) for the truncated scattering transform $\mathbf{t}_R^\varepsilon(k)$. Using (1.10) to write

$$\frac{\mathbf{t}_R^\varepsilon(k)}{\bar{k}} = \frac{1}{\bar{k}} \int_{\partial\mathbb{D}} e^{i\bar{k}\bar{x}} (\Lambda_\gamma^\varepsilon - \Lambda_1) \psi^\varepsilon(\cdot, k) d\sigma = \int_{\partial\mathbb{D}} \frac{e^{i\bar{k}\bar{x}} - 1}{\bar{k}} (\Lambda_\gamma^\varepsilon - \Lambda_1) \psi^\varepsilon(\cdot, k) d\sigma$$

shows that $\mathbf{t}_R^\varepsilon(k)/\bar{k}$ is bounded and continuous for $|k| < R(\varepsilon)$. Hence by Theorem 4.1 of [71] the integral equation (1.17) has a unique solution. Thus $\Gamma_{\alpha(\varepsilon)}\Lambda_\gamma^\varepsilon$ is well-defined by (1.18) with the choice $\alpha(\varepsilon) = 1/R(\varepsilon)$.

Let $\gamma \in \mathcal{D}(F)$ fixed. Note that the *a priori* condition (1.6) gives upper bounds for the $L^p(\mathbb{R}^2)$ norms of the scattering transforms $\mathbf{t}(k)$ and $\mathbf{t}_R^\varepsilon(k)$. Using Lemma 2.1 in the case $\phi_2 = 0$ and $\mu_2 \equiv 1$ yields the following two inequalities:

$$\|\mu(\cdot, 0)\|_{L^\infty(\mathbb{D})} \leq C(M, \rho), \quad \|\mu_R^\varepsilon(\cdot, 0)\|_{L^\infty(\mathbb{D})} \leq C(M, \rho).$$

Thus we may estimate

$$\begin{aligned} \|\Gamma_{\alpha(\varepsilon)}\Lambda_\gamma^\varepsilon - \gamma\|_{L^\infty(\mathbb{D})} &= \|\mu(\cdot, 0)^2 - \mu_R^\varepsilon(\cdot, 0)^2\|_{L^\infty(\mathbb{D})} \\ &= \|(\mu(\cdot, 0) - \mu_R^\varepsilon(\cdot, 0))(\mu(\cdot, 0) + \mu_R^\varepsilon(\cdot, 0))\|_{L^\infty(\mathbb{D})} \\ &\leq C\|\mu(\cdot, 0) - \mu_R^\varepsilon(\cdot, 0)\|_{L^\infty(\mathbb{D})}, \end{aligned}$$

so it is enough to show $\|\mu(\cdot, 0) - \mu_R^\varepsilon(\cdot, 0)\|_{L^\infty(\mathbb{D})} \leq C(-\log \varepsilon)^{-1/14}$.

Take $p = 7/5$. We define p' and \tilde{p} and p_1 by the formulae

$$\frac{1}{p} + \frac{1}{p'} = 1, \quad \frac{1}{\tilde{p}} = \frac{1}{p} - \frac{1}{2}, \quad \frac{1}{p_1} = \frac{1}{p} - \frac{1}{p'}.$$

Then

$$p' = \frac{7}{2}, \quad \tilde{p} = \frac{14}{3}, \quad \tilde{p}' = \frac{14}{11}, \quad p_1 = \frac{7}{3}.$$

Estimate using Lemma 2.1

$$\begin{aligned} \|\mu(x, \cdot) - \mu_R^\varepsilon(x, \cdot)\|_{C^\alpha(\mathbb{R}^2)} &\leq C \left\| \frac{\mathbf{t}(k) - \mathbf{t}_R^\varepsilon(k)}{\bar{k}} \right\|_{L^p \cap L^{p'}(|k| < R)} \\ (3.2) \quad &+ C \left\| \frac{\mathbf{t}(k)}{\bar{k}} \right\|_{L^p(|k| > R)}. \end{aligned}$$

Then Lemma 2.4 shows that

$$(3.3) \quad \left\| \frac{\mathbf{t}(k) - \mathbf{t}_R^\varepsilon(k)}{\bar{k}} \right\|_{L^p \cap L^{p'}(|k| < R)} \leq C(-\log \varepsilon)^{10/7} \varepsilon^{1/10},$$

so it remains to bound the second term in the right hand side of (3.2).

Write $q = \gamma^{-1/2} \Delta \gamma$ and decompose \mathbf{t} as

$$(3.4) \quad \mathbf{t}(k) = (\mathcal{F}q)(k) + \mathcal{F}(q(\mu(\cdot, k) - 1))(k).$$

We need the norm estimate [71, formula (1.1)] in the form

$$(3.5) \quad \|\mu(\cdot, k) - 1\|_{W^{1/2, \tilde{p}}(\mathbb{R}^2)} \leq C|k|^{-1/2} \|q\|_{L^p(\mathbb{R}^2)}.$$

As in the proof of Lemma 2.6 in [72], estimate (3.5) implies that there exists some $R_0 > 0$ such that for $|k| > R_0$ we have the estimate

$$\begin{aligned} |\mathcal{F}(q(\mu(\cdot, k) - 1))(k)| &\leq \|q\|_{L^1(\mathbb{R}^2)} \|\mu(\cdot, k) - 1\|_{W^{1/2, \tilde{p}}(\mathbb{R}^2)} \\ &\leq C\|q\|_{L^1(\mathbb{R}^2)} \|q\|_{L^p(\mathbb{R}^2)} |k|^{-1/2} \\ (3.6) \quad &\leq C|k|^{-1/2}, \end{aligned}$$

where the constant C depends on M . Thus we get using (3.6)

$$(3.7) \quad \left\| \frac{\mathcal{F}(q(\mu(\cdot, k) - 1))(k)}{\bar{k}} \right\|_{L^p(|k| > R)} \leq C \left(\int_R^\infty r^{-\frac{21}{10}+1} dr \right)^{5/7} = CR^{-1/14}.$$

By Hölder's inequality and the Riesz-Thorin interpolation theorem

$$\begin{aligned}
\left\| \frac{(\mathcal{F}q)(k)}{\bar{k}} \right\|_{L^p(|k|>R)} &\leq \| \mathcal{F}q \|_{L^{p'}(\mathbb{R}^2)} \| k^{-1} \|_{L^{p_1}(|k|>R)} \\
&\leq \| q \|_{L^p(\mathbb{R}^2)} \left(2\pi \int_R^\infty r^{-\frac{7}{3}+1} dr \right)^{3/7} \\
(3.8) \qquad \qquad \qquad &\leq CR^{-1/7},
\end{aligned}$$

where the constant C depends on M . Now formulae (3.7) and (3.8) imply

$$C \left\| \frac{\mathbf{t}(k)}{\bar{k}} \right\|_{L^p(|k|>R)} \leq C(-\log \varepsilon)^{-1/7} + C(-\log \varepsilon)^{-1/14},$$

and estimate (3.1) follows. \square

The above result is not enough to show that the family Γ_α would be a regularization strategy for F : according to Definition 1.2, the map Γ_α should be defined and continuous on the whole data space Y . Theorem 3.1 only defines Γ_α in an ε_0 -neighborhood of the subset $F(\mathcal{D}(F)) \subset Y$, and the structure of $F(\mathcal{D}(F))$ is related to the notoriously difficult open problem of characterizing the range of F .

We proceed by defining an extended regularization strategy $\tilde{\Gamma}_\alpha$ that is well-defined and continuous on Y and coincides with Γ_α near $F(\mathcal{D}(F))$ when α is small. The main difficulty is extending Step 1 $^\varepsilon$ for large ε as the operator $B_k^\varepsilon = I + S_k(\Lambda_\gamma^\varepsilon - \Lambda_1)$ is not necessarily invertible in that case. We overcome this problem by constructing a generally applicable approximate inverse for B_k^ε .

Let $(B_k^\varepsilon)^*$ be the adjoint operator of $B_k^\varepsilon \in \mathcal{L}(H^{1/2}(\partial\mathbb{D}))$, and define

$$T_k^\varepsilon := (B_k^\varepsilon)^* B_k^\varepsilon \in \mathcal{L}(H^{1/2}(\partial\mathbb{D})).$$

We denote the spectrum of T_k^ε by $\sigma(T_k^\varepsilon)$. Since T_k^ε is a self-adjoint operator in $H^{1/2}(\partial\mathbb{D})$, there exists spectral resolution [91]

$$T_k^\varepsilon = \int_{\sigma(T_k^\varepsilon)} \lambda dP(\lambda).$$

The α -pseudoinverse $(B_k^\varepsilon)_\alpha^\dagger$ of B_k^ε is defined for any $0 < \alpha < \infty$ by

$$(3.9) \qquad (B_k^\varepsilon)_\alpha^\dagger := h_\alpha(T_k^\varepsilon)(B_k^\varepsilon)^*,$$

where

$$(3.10) \qquad h_\alpha(T_k^\varepsilon) = \int_{\sigma(T_k^\varepsilon)} h_\alpha(\lambda) dP(\lambda),$$

and the function $h_\alpha : \mathbb{R} \rightarrow \mathbb{R}$ is defined for all $0 < \alpha < \infty$ by

$$(3.11) \qquad h_\alpha(t) := \begin{cases} t^{-1} & \text{for } t > \kappa(\alpha), \\ \kappa(\alpha)^{-1} & \text{for } t \leq \kappa(\alpha). \end{cases}$$

The definition of $\kappa(\alpha) > 0$ in (3.11) involves the constant C_2 defined in the proof of Lemma 2.3:

$$(3.12) \qquad \kappa(\alpha) := \frac{1}{4} \left(\frac{e^{-2/\alpha}}{C_2(1+1/\alpha)} \right)^2.$$

Now the following lemma shows that the α -pseudoinverse $(B_k^\varepsilon)^\dagger_\alpha$ depends continuously on \mathcal{E} :

Lemma 3.1. *The operator $h_\alpha(T)$ depends continuously in $\mathcal{L}(H^{1/2}(\partial\mathbb{D}))$ on the selfadjoint operator $T \in \mathcal{L}(H^{1/2}(\partial\mathbb{D}))$.*

Proof. Let $T \in \mathcal{L}(H^{1/2}(\partial\mathbb{D}))$ be a selfadjoint operator, $b = \|T\|_{\mathcal{L}(H^{1/2}(\partial\mathbb{D}))}$, and $\mathcal{K} \subset \mathcal{L}(H^{1/2}(\partial\mathbb{D}))$ be the set of selfadjoint operators T' satisfying $\|T' - T\|_{\mathcal{L}(H^{1/2}(\partial\mathbb{D}))} < 1$. By the Weierstrass theorem, there are polynomials $p_n(z)$ such that

$$(3.13) \quad \lim_{n \rightarrow \infty} \|p_n - h_\alpha\|_{C([-b, b])} = 0.$$

As $\sigma(T') \subset [-b - 1, b + 1]$, formula (3.13) and spectral theory imply that

$$(3.14) \quad \lim_{n \rightarrow \infty} \|p_n(T') - h_\alpha(T')\|_{\mathcal{L}(H^{1/2}(\partial\mathbb{D}))} = 0$$

uniformly in $T' \in \mathcal{K}$. Now

$$p_n(T') = \frac{1}{2\pi i} \int_c p_n(z)(T' - z)^{-1} dz,$$

where c is the circle in \mathbb{C} with center zero and radius $b + 2$ and oriented in counterclockwise direction. Using the fact that the distance of the spectrum of the selfadjoint operator T' to c is bounded by one, [46, Thm. IV.1.16] implies that $(T', z) \mapsto (T' - z)^{-1}$ is a uniformly continuous map from $\mathcal{K} \times c$ to $\mathcal{L}(H^{1/2}(\partial\mathbb{D}))$. Thus $T' \mapsto p_n(T')$ is continuous from \mathcal{K} to $\mathcal{L}(H^{1/2}(\partial\mathbb{D}))$ for each n . Applying (3.14), we see that $T' \mapsto h_\alpha(T')$ is continuous from \mathcal{K} to $\mathcal{L}(H^{1/2}(\partial\mathbb{D}))$. \square

We are ready to define the extended regularization strategy $\tilde{\Gamma}_\alpha$.

Step 1 $_\alpha$: From noisy data $\Lambda_\gamma^\varepsilon$ to scattering transform $\tilde{\mathbf{t}}_\alpha$. Given $\alpha > 0$, use (3.9) to define $\tilde{\psi}_\alpha := (B_k^\varepsilon)^\dagger_\alpha(e^{ikx}|_{\partial\mathbb{D}})$ for $|k| < R(\alpha) = 1/\alpha$, and substitute the result to the formula

$$(3.15) \quad \tilde{\mathbf{t}}_\alpha(k) = \begin{cases} \int_{\partial\mathbb{D}} e^{ik\bar{x}} (\Lambda_\gamma^\varepsilon - \Lambda_1) \tilde{\psi}_\alpha(\cdot, k) d\sigma & \text{for } |k| < R(\alpha), \\ 0, & \text{otherwise.} \end{cases}$$

Step 2 $_\alpha$: From $\tilde{\mathbf{t}}_\alpha$ to reconstruction $\tilde{\Gamma}_\alpha \Lambda_\gamma^\varepsilon$. For each fixed $x \in \mathbb{D}$, solve

$$\tilde{\mu}_\alpha(x, k) = 1 + \frac{1}{(2\pi)^2} \int_{|k'| < R(\alpha)} \frac{\tilde{\mathbf{t}}_\alpha(k')}{(k - k')\bar{k}'} e_{-x}(k') \overline{\tilde{\mu}_\alpha(x, k')} dk'_1 dk'_2,$$

and set

$$(3.16) \quad (\tilde{\Gamma}_\alpha \Lambda_\gamma^\varepsilon)(x) := (\tilde{\mu}_\alpha(x, 0))^2.$$

Finally, we prove that $\tilde{\Gamma}_\alpha$ is a regularization strategy.

Theorem 3.2. *Let \mathbb{D} be the unit disk. Assume $M > 0$ and $0 < \rho < 1$ are given, let $\mathcal{D}(F)$ be as in Definition 1.1, and let $\varepsilon_0 > 0$ be as in Theorem 3.1. Then the family $\tilde{\Gamma}_\alpha$ defined by (3.16) is a regularization strategy for F in the sense of Definition 1.2 with the following admissible choice of regularization parameter:*

$$(3.17) \quad \alpha(\varepsilon) = \begin{cases} -\frac{10}{\log \varepsilon}, & \text{for } 0 < \varepsilon < \varepsilon_0, \\ -\frac{10\varepsilon}{\varepsilon_0 \log \varepsilon_0}, & \text{for } \varepsilon \geq \varepsilon_0. \end{cases}$$

Proof. It is clear from the above construction and Proposition 3.5 of [53] that $\tilde{\Gamma}_\alpha : Y \rightarrow C^2(\overline{\mathbb{D}}) \subset L^\infty(\mathbb{D})$ is a well-defined and continuous mapping.

Recall that the operator $B_k = I + S_k(\Lambda_\gamma - \Lambda_1) \in \mathcal{L}(H^{1/2}(\partial\mathbb{D}))$ is invertible for all $\gamma \in \mathcal{D}(F)$ by [71]. Furthermore, take C_2 as in Lemma 2.3 and define

$$r(\alpha) := \frac{e^{-2/\alpha}}{C_2(1+1/\alpha)},$$

where C_2 depends only on the *a priori* information M, ρ ; then by Lemma 2.3

$$\|B_k^{-1}\|_{\mathcal{L}(H^{1/2}(\partial\mathbb{D}))} \leq r(\alpha)^{-1}$$

for all $\gamma \in \mathcal{D}(F)$ and $|k| < 1/\alpha$.

Write $A_k^\varepsilon = S_k \mathcal{E} B_k^{-1}$; then $B_k^\varepsilon = [I + A_k^\varepsilon] B_k$. We know from the proof of Lemma 2.4 that $\|A_k^\varepsilon\|_{1/2} < \frac{1}{2}$ whenever $0 < \varepsilon < \varepsilon_0$ and $|k| < 1/\alpha(\varepsilon)$. We see that

$$\|(B_k^\varepsilon)^{-1}\|_{\mathcal{L}(H^{1/2}(\partial\mathbb{D}))} \leq \|B_k^{-1}\|_{\mathcal{L}(H^{1/2}(\partial\mathbb{D}))} \|(I + A_k^\varepsilon)^{-1}\|_{\mathcal{L}(H^{1/2}(\partial\mathbb{D}))}$$

for all $\gamma \in \mathcal{D}(F)$ and $0 < \varepsilon < \varepsilon_0$ and $|k| < 1/\alpha$. Thus

$$T_k^\varepsilon = (B_k^\varepsilon)^* B_k^\varepsilon \geq \frac{r(\alpha)^2}{4} I.$$

Recall that the α -pseudoinverse is defined in (3.10), (3.11) and (3.12) where $\kappa(\alpha) = \frac{r(\alpha)^2}{4}$. Then for $|k| < 1/\alpha$ we have $h_\alpha(T_k^\varepsilon) = (T_k^\varepsilon)^{-1}$ and consequently

$$(3.18) \quad (B_k^\varepsilon)^\dagger_\alpha = (B_k^\varepsilon)^{-1}.$$

Now we have by (3.18) that $\tilde{\psi}_{\alpha(\varepsilon)} = \psi^\varepsilon$ and thus for small enough ε the formulae (1.16) and (3.15) coincide.

Property (1.13) is clear from (3.17), and Theorem 3.1 implies (1.12) and (1.14). \square

We remark that there are many equally plausible ways to define $\alpha(\varepsilon)$; the crucial properties of formula (3.17) are that α is continuous in ε and $\lim_{\varepsilon \rightarrow \infty} \alpha(\varepsilon) = \infty$.

4. COMPUTATIONAL METHODS

In this section we simulate EIT data with various degrees of noise and present a computational study of the regularized EIT imaging method outlined above. It is essential to our constructions that $\mathbb{D} \subset \mathbb{R}^2$ is the unit disc.

4.1. Practical representation of Sobolev spaces at the boundary. Denote by $\mathcal{S} := C^\infty(\partial\mathbb{D})$ the space of smooth test functions defined on the boundary $\partial\mathbb{D}$. We define Fourier series for $f \in \mathcal{S}$ by the formula

$$(4.1) \quad \hat{f}(\ell) := \frac{1}{\sqrt{2\pi}} \int_0^{2\pi} f(\theta) e^{-i\ell\theta} d\theta, \quad \ell \in \mathbb{Z}.$$

Definition (4.1) extends to the space \mathcal{S}' of distributions in the standard way.

We proceed to give explicit definitions of Hilbert space inner products and norms for the Sobolev spaces $H^s(\partial\mathbb{D})$ with $s \in \mathbb{R}$. Set

$$(4.2) \quad \langle f, g \rangle_s := \langle f, g \rangle_{H^s(\partial\mathbb{D})} = \sum_{\ell \in \mathbb{Z}} w_s(\ell) \hat{f}(\ell) \overline{w_s(\ell) \hat{g}(\ell)},$$

where $s \in \mathbb{R}$, $\ell \in \mathbb{Z}$, and the multiplier function is defined by

$$(4.3) \quad w_s(\ell) := (1 + |\ell|^2)^{s/2} \quad \text{for } s \in \mathbb{R}, \ell \in \mathbb{Z}.$$

In the sequel we denote $\|f\|_s = \|f\|_{H^s(\partial\mathbb{D})} = \langle f, f \rangle_s^{1/2}$.

Next we build an orthonormal basis for the Hilbert space $H^s(\partial\mathbb{D})$. Define

$$(4.4) \quad \phi_n^s(\theta) = \frac{w_{-s}(n)}{\sqrt{2\pi}} e^{in\theta},$$

and compute the Fourier coefficients of the functions ϕ_n^s by (4.1) for later reference:

$$(4.5) \quad \widehat{\phi_n^s}(\ell) = \frac{w_{-s}(n)}{2\pi} \int_0^{2\pi} e^{i(n-\ell)\theta} d\theta = w_{-s}(n) \delta_n(\ell),$$

where $\delta_n(\ell) = 1$ when $n = \ell$ and zero otherwise.

In practical computations one needs to truncate the basis. Given an integer $N > 0$ we approximate a function $f \in H^s(\partial\mathbb{D})$ and its norm by

$$(4.6) \quad f(\theta) \approx \sum_{n=-N}^N \langle f, \phi_n^s \rangle_s \phi_n^s(\theta), \quad \|f\|_s \approx \left(\sum_{n=-N}^N |\langle f, \phi_n^s \rangle_s|^2 \right)^{1/2}.$$

4.2. Numerical representation of operators. Assume we are given a linear operator $\mathcal{A} : \mathcal{S} \rightarrow \mathcal{S}$. Relevant examples of such operators include $\Lambda_\gamma^\varepsilon, \Lambda_1$ and S_k related to the boundary integral equation (1.15).

Given $N > 0$, we define a matrix $A : \mathbb{C}^{2N+1} \rightarrow \mathbb{C}^{2N+1}$ by $A := [A_{mn}]$ with

$$(4.7) \quad A_{mn} := \frac{1}{2\pi} \int_0^{2\pi} (\mathcal{A}e^{in\theta}) e^{-im\theta} d\theta.$$

Here $m \in \{-N, \dots, N\}$ is the row index and $n \in \{-N, \dots, N\}$ is the column index. We will use matrices of the form (4.7) below for numerical solution of (1.15).

Below we will need to compute the Y -norm of the measurement error $\mathcal{E} = \Lambda_\gamma - \Lambda_\gamma^\varepsilon$ approximately from matrix representations. Now $\mathcal{E} : H^s(\partial\mathbb{D}) \rightarrow H^{-s}(\partial\mathbb{D})$ is a bounded linear operator with norm

$$(4.8) \quad \|\mathcal{E}\|_{\mathcal{L}(H^s, H^{-s})} = \sup_{f \in H^s} \frac{\|\mathcal{E}f\|_{-s}}{\|f\|_s}.$$

We approximate $\|\mathcal{E}\|_{\mathcal{L}(H^s, H^{-s})}$ numerically by substituting $\mathcal{E}f$ and f in the right-hand side of (4.8) by finite-dimensional approximations as in (4.6).

Define vectors $\vec{f} \in \mathbb{C}^{2N+1}$ and $\vec{e} \in \mathbb{C}^{2N+1}$ as follows:

$$\vec{f} = \begin{bmatrix} \langle f, \phi_{-N}^s \rangle_s \\ \vdots \\ \langle f, \phi_0^s \rangle_s \\ \vdots \\ \langle f, \phi_N^s \rangle_s \end{bmatrix}, \quad \vec{e} = \begin{bmatrix} \langle \mathcal{E}f, \phi_{-N}^{-s} \rangle_{-s} \\ \vdots \\ \langle \mathcal{E}f, \phi_0^{-s} \rangle_{-s} \\ \vdots \\ \langle \mathcal{E}f, \phi_N^{-s} \rangle_{-s} \end{bmatrix}.$$

Then we can use Euclidean norms according to (4.6):

$$(4.9) \quad \|f\|_s \approx \|\vec{f}\|_{\mathbb{C}^{2N+1}}, \quad \|\mathcal{E}f\|_{-s} \approx \|\vec{e}\|_{\mathbb{C}^{2N+1}}.$$

Let us compute

$$\begin{aligned}\langle \mathcal{E}f, \phi_m^{-s} \rangle_{-s} &= \left\langle \mathcal{E} \left(\sum_{n=-N}^N \langle f, \phi_n^s \rangle_s \phi_n^s(\theta) \right), \phi_m^{-s} \right\rangle_{-s} \\ &= \sum_{n=-N}^N \langle f, \phi_n^s \rangle_s \langle \mathcal{E} \phi_n^s, \phi_m^{-s} \rangle_{-s},\end{aligned}$$

so defining a $(2N+1) \times (2N+1)$ matrix $B = [B(m, n)] := [\langle \mathcal{E} \phi_n^s, \phi_m^{-s} \rangle_{-s}]$ yields

$$(4.10) \quad \vec{e} = B\vec{f}.$$

Now combining (4.8), (4.9) and (4.10) yields

$$(4.11) \quad \|\mathcal{E}\|_{\mathcal{L}(H^s, H^{-s})} \approx \sup_{\vec{f} \in \mathbb{C}^{2N+1}} \frac{\|B\vec{f}\|_{\mathbb{C}^{2N+1}}}{\|\vec{f}\|_{\mathbb{C}^{2N+1}}} = \|B\|_{\mathbb{C}^{2N+1} \rightarrow \mathbb{C}^{2N+1}},$$

where $\|B\|_{\mathbb{C}^{2N+1} \rightarrow \mathbb{C}^{2N+1}}$ is standard matrix operator norm.

Let us determine the matrix element $B(m, n) = \langle \mathcal{E} \phi_n^s, \phi_m^{-s} \rangle_{-s}$ in terms of the matrix approximation E_{mn} defined by (4.7) for \mathcal{E} . Truncate formula (4.2) and apply (4.5) and (4.1) to get

$$\begin{aligned}\langle \mathcal{E} \phi_n^s, \phi_m^{-s} \rangle_{-s} &\approx \sum_{\ell=-N}^N w_{-s}(\ell) \widehat{\mathcal{E} \phi_n^s}(\ell) \overline{w_{-s}(\ell) \widehat{\phi_m^{-s}}(\ell)} \\ &= w_{-s}(m) \widehat{\mathcal{E} \phi_n^s}(m) \\ &= w_{-s}(m) w_{-s}(n) \frac{1}{2\pi} \int_0^{2\pi} (\mathcal{E} e^{in\theta}) e^{-im\theta} d\theta \\ &= w_{-s}(m) w_{-s}(n) E_{mn}.\end{aligned}$$

Finally, (4.11) takes the form

$$(4.12) \quad \|\mathcal{E}\|_{\mathcal{L}(H^s, H^{-s})} \approx \|[w_{-s}(m) w_{-s}(n) E_{mn}]\|_{\mathbb{C}^{2N+1} \rightarrow \mathbb{C}^{2N+1}}.$$

4.3. Simulation of noisy measurement data. In this section we will construct a matrix approximation to a noisy Dirichlet-to-Neumann operator $\Lambda_\gamma^\varepsilon$. Let $\mathcal{R}_\gamma : \widetilde{H}^{-1/2}(\partial\mathbb{D}) \rightarrow \widetilde{H}^{1/2}(\partial\mathbb{D})$ denote the Neumann-to-Dirichlet map of γ , where \widetilde{H}^s spaces consist of H^s functions with mean value zero. A method for approximating \mathcal{R}_γ and $\Lambda_\gamma^\varepsilon$ from experimental data can be found, for example, in [41]. In practice, contributions to the noise come from noise in the input current, measured voltages, and modeling errors such as the approximation of an infinite dimensional operator by a discrete matrix. Bounds for the contributions to the noise from the hardware are usually known, but contributions from the modeling are more difficult to quantify, and we do not address that problem here.

Let u be the unique $H^1(\mathbb{D})$ solution of the Neumann problem

$$(4.13) \quad \nabla \cdot \gamma \nabla u = 0 \text{ in } \mathbb{D}, \quad \gamma \frac{\partial u}{\partial \nu} = g \text{ on } \partial\mathbb{D},$$

satisfying $\int_{\partial\mathbb{D}} u d\sigma = 0$. Then we have $\mathcal{R}_\gamma g = u|_{\partial\mathbb{D}}$. We note two key equalities concerning Λ_γ and \mathcal{R}_γ . Define a projection operator $P\phi := |\partial\mathbb{D}|^{-1} \int_{\partial\mathbb{D}} \phi$. Then for

any $f \in H^{1/2}(\partial\mathbb{D})$ we have $P\Lambda_\gamma f = |\partial\mathbb{D}|^{-1} \int_{\partial\mathbb{D}} \gamma \frac{\partial u}{\partial \nu} = \int_{\mathbb{D}} \nabla \cdot \gamma \nabla u = 0$, so actually $\Lambda_\gamma : H^{1/2}(\partial\mathbb{D}) \rightarrow \tilde{H}^{-1/2}(\partial\mathbb{D})$. From the definitions of Λ_γ and \mathcal{R}_γ we now have

$$(4.14) \quad \Lambda_\gamma \mathcal{R}_\gamma = I \quad : \tilde{H}^{-1/2}(\partial\mathbb{D}) \rightarrow \tilde{H}^{-1/2}(\partial\mathbb{D}),$$

$$(4.15) \quad \mathcal{R}_\gamma \Lambda_\gamma = I - P \quad : H^{1/2}(\partial\mathbb{D}) \rightarrow \tilde{H}^{1/2}(\partial\mathbb{D}).$$

Given γ and $N > 0$, we define a matrix $R_\gamma : \mathbb{C}^{2N} \rightarrow \mathbb{C}^{2N}$ as follows. For each $n = -N, -N+1, \dots, -1, 1, \dots, N$ note that $\int_{\partial\mathbb{D}} \mathbb{D} \phi_n d\sigma = 0$. Then solve the Neumann problem

$$(4.16) \quad \nabla \cdot \gamma \nabla u_n = 0 \text{ in } \mathbb{D}, \quad \gamma \frac{\partial u_n}{\partial \nu} = \phi_n \text{ on } \partial\mathbb{D},$$

with the constraint $\int_{\partial\mathbb{D}} \mathbb{D} u_n d\sigma = 0$. Thus $R_\gamma = [\hat{u}_n(\ell)]$ with

$$(4.17) \quad \hat{u}_n(\ell) = \int_{\partial\mathbb{D}} u_n \bar{\phi}_\ell d\sigma.$$

Here ℓ is row index and n is column index.

The matrix R_γ represents the operator \mathcal{R}_γ approximately. We can now easily compute the corresponding matrix representation L_γ for the DN map Λ_γ . Namely, define

$$L'_\gamma := R_\gamma^{-1};$$

then L'_γ is a matrix of size $2N \times 2N$. We should add appropriate mapping properties for constant basis functions at the boundary according to the facts

$$\Lambda_\gamma 1 = 0, \quad \int_{\partial\mathbb{D}} \Lambda_\gamma f d\sigma = 0.$$

This is achieved simply by setting (in Matlab notation)

$$(4.18) \quad L_\gamma = \begin{bmatrix} L'_\gamma(1:N, 1:N) & 0 & L'_\gamma(1:N, (N+1):\text{end}) \\ 0 & 0 & 0 \\ L'_\gamma((N+1):\text{end}, 1:N) & 0 & L'_\gamma((N+1):\text{end}, (N+1):\text{end}) \end{bmatrix}$$

the zero block matrices above have various (but obvious) sizes.

We add simulated measurement noise of amplitude $\varepsilon > 0$ by first defining

$$L''_\gamma := L'_\gamma + cE,$$

where E is a $2N \times 2N$ matrix with random entries independently distributed according to the Gaussian normal density $\mathcal{N}(0, 1)$. We enforce self-adjointness by setting

$$L'''_\gamma := \frac{1}{2}(L''_\gamma + (L''_\gamma)^H),$$

and the constant $c > 0$ is adjusted so that $\|L'_\gamma - L'''_\gamma\|_{2,2} = \varepsilon$; then we define noisy data by replacing L'_γ by L'''_γ in formula (4.18). Then we can consider the matrix cE as an approximation of a continuous operator \mathcal{E} with $\|\mathcal{E}\|_Y \approx \varepsilon$. Note that the zero blocks in (4.18) take care of the requirements $\mathcal{E}1 = 0$ and $\int_{\partial\mathbb{D}} \mathcal{E} f d\sigma = 0$.

4.4. Solving the boundary integral equation. We explain how to solve equation (1.15) approximately by numerical computation.

Choose $N > 0$. We showed in Section 4.3 how to express $\Lambda_\gamma^\varepsilon$ and Λ_1 as matrices in Fourier basis. It remains to write the operator S_k as a matrix in the same basis. Recall the decomposition (2.7). In our case of \mathbb{D} being the unit disc, the standard single layer operator $S_0 = \frac{1}{2}R_1$ (see e.g. [82]) and hence has the matrix

$$\frac{1}{2}\text{diag}\left[\frac{1}{N}, \frac{1}{N-1}, \dots, \frac{1}{2}, 1, 0, 1, \frac{1}{2}, \dots, \frac{1}{N-1}, \frac{1}{N}\right].$$

The third term in (2.7) does not contribute to equation (1.15) at all since

$$\int_{\partial\mathbb{D}} (\Lambda_\gamma^\varepsilon f)(y) d\sigma(y) = 0 = \int_{\partial\mathbb{D}} (\Lambda_1 f)(y) d\sigma(y),$$

the former equation by assumptions $\mathcal{E} \in Y$ and (1.10).

It remains to find a matrix for the operator \mathcal{H}_k defined by

$$\mathcal{H}_k \phi(x) := \int_{\partial\mathbb{D}} H_1(k(x-y)) \phi(y) d\sigma(y).$$

Now \mathcal{H}_k can be written in matrix form using (4.7) and a numerical evaluation routine for the function $H_1(x)$. Such a routine in turn relies by (2.5) on numerical evaluation of Faddeev's fundamental solution $g_1(x)$. An algorithm for computing g_1 was introduced in [81] and later refined in [40].

Approximate solution of (1.15) is now given by expanding $e^{ikx}|_{\partial\mathbb{D}}$ as a vector g in our truncated Fourier basis and setting

$$(4.19) \quad \tilde{\psi}_R := [I + S_k(\Lambda_\gamma^\varepsilon - \Lambda_1)]^{-1} g.$$

According to the theory, the inverse matrix $[I + S_k(\Lambda_\gamma^\varepsilon - \Lambda_1)]^{-1}$ exists for all k in some disc $D(0, R)$, at least when the order N of trigonometric approximation is high enough.

5. REGULARIZED RECONSTRUCTIONS

We construct a $C^2(\mathbb{D})$ function that models roughly a two-dimensional transverse cross-section through a human chest, see Figure 1. The background conductivity equals one, and there is a narrow neighborhood of the boundary where $\gamma \equiv 1$ according to the assumptions of the theory. The lungs are modeled by two low-conductivity regions with minimum conductivity 0.5. The heart is modeled by a high-conductivity region with maximum conductivity 2.

The scattering transform $\mathbf{t}(k)$ for $|k| \leq 10$ is computed numerically as explained in [67, section 3.1]. This is done for

- assessing the quality of scattering transforms computed from simulated boundary measurements, and
- choosing the regularization parameter in our numerical example (we stress that this cannot be done in practical situations; below such a step is used for illustrating optimal behaviour of the proposed regularization method).

Let us summarize the computation briefly: we use numerical differentiation to find $q(x) = \gamma^{-1/2} \Delta \gamma^{1/2}$, solve the Lippmann-Schwinger type equation $\mu = 1 - g_k * (q\mu)$ using periodization, and integrate numerically to get

$$\mathbf{t}(k) = \int_{\text{supp } q} e^{i(kx + \bar{k}\bar{x})} q(x) \mu(x, k) dx.$$

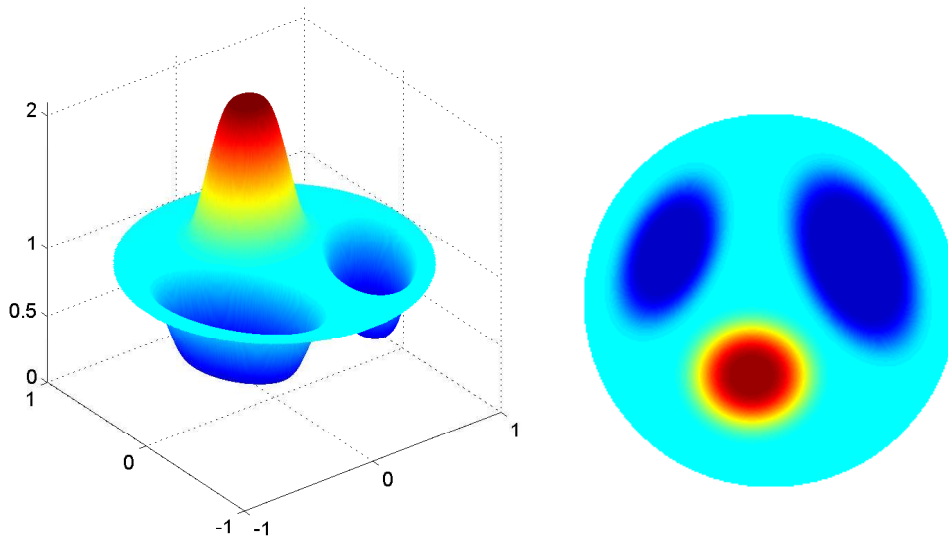


FIGURE 1. Simulated phantom modeling transverse cross-section of human chest. Left: three-dimensional plot. Right: color image. The color scale is the same in both plots.

This definition is consistent with (1.4). Note that this computation is not directly related to the inverse problem since we use the knowledge of γ inside \mathbb{D} which is not available in practice.

The noisy Dirichlet-to-Neumann maps are simulated as explained in Section 4.3. The Neumann problem (4.13) is solved numerically using the finite element method as provided by the PDE toolbox of Matlab. We add simulated data of amplitudes $\|\mathcal{E}\|_Y \approx 10^{-2}, 10^{-3}, 10^{-4}, 10^{-5}$, and numerical tests show that numerical error in the map Λ_γ resulting from finite element method is roughly $\|\mathcal{E}\|_Y \approx 10^{-6}$. Also, it turns out that for our phantom $\|\Lambda_\gamma\|_Y = 0.9989 \approx 1$, so the relative errors can be calculated simply by $\|\mathcal{E}\|_Y / \|\Lambda_\gamma\|_Y \approx \|\mathcal{E}\|_Y$.

We solve the boundary integral for $\tilde{\psi}_R$ by formula (4.19). It turns out that the inverse matrix $[I + S_k(\Lambda_\gamma - \Lambda_1)]^{-1}$ does exist for all k in $D(0, 10)$. We continue by writing

$$\tilde{\mathbf{t}}_R(k) := \int_{\partial\mathbb{D}} e^{i\bar{k}\bar{x}} (\Lambda_\gamma - \Lambda_1) \tilde{\psi}_R(\cdot, k) d\sigma(x)$$

and find out numerically that

$$(5.1) \quad |\tilde{\mathbf{t}}_R(k) - \mathbf{t}(k)| \leq 1 \quad \text{when } |k| \leq 6.7.$$

This observation leads us to choose $R = 6.7$ for the truncation radius corresponding to the DN map provided by our finite element solver without simulated noise added. Further, we add various levels of noise and observe that the bound for $|k|$ in (5.1) decreases as the noise level increases. We continue to choose R based on the threshold 1 for the absolute difference between $\tilde{\mathbf{t}}_R$ and \mathbf{t} . The choice of R used in each reconstruction is given in figure 2. Note that the truncation radius R chosen by the criterion (5.1) is significantly larger than the choice dictated by Lemma 2.4; see Figure 3 for a quantitative comparison.

The above choice of truncation radius is dubious in at least two ways. First, in practical cases we do not have \mathbf{t} available for comparison since the unknown conductivity is needed for the computation of \mathbf{t} . Second, the choice of 1 as the threshold is arbitrary (it represents roughly 10% pointwise absolute error in $\tilde{\mathbf{t}}_R$). However, any practical method for determining R has to rely on some criterion for deciding for how large $|k|$ does the noise level prevent good enough quality in recovered $\tilde{\mathbf{t}}_R$.

We do not discuss automatic choice of truncation radius R in this work. Such a choice is comparable in complexity to the notoriously difficult (and largely open) problem of finding the regularization parameter automatically for Tikhonov regularization.

Having computed $\tilde{\mathbf{t}}_R(k)$ in a disc $|k| \leq R$ we substitute it as kernel in the D-bar equation and reconstruct the conductivity approximately using the numerical solver introduced in [54]. The computation was performed in parallel on a PC grid provided by Techila Technologies Ltd. Parallelization speeded up the computations by a factor of 100 as compared to solution using just one PC computer. See Figure 2 for reconstructions at various noise levels.

Finally, we present a couple of reconstructions using the Born approximation as was done in [82, 68, 67, 41, 42, 53, 52]. This is to provide the reader a possibility to compare the new regularized algorithm to the previously established approach. The truncated kernel for the $\bar{\partial}$ equation is computed with the formula

$$(5.2) \quad \mathbf{t}_R^{\text{exp}}(k) = \begin{cases} \int_{\partial\mathbb{D}} e^{i\bar{k}\bar{x}} (\Lambda_\gamma^\varepsilon - \Lambda_1) e^{ikx} d\sigma & \text{for } |k| < R, \\ 0, & \text{otherwise.} \end{cases}$$

We used the data set with the least amount of noise ($\|\mathcal{E}\|_Y \approx 10^{-6}$). Truncation radius $R = 6.7$ was found to be too large as it leads to severe artefacts, see the left plot in Figure 4. We chose another truncation radius $R = 4.5$ based on visually inspecting the graph of $\mathbf{t}_R^{\text{exp}}$ and choosing the largest R retaining reasonable numerical accuracy inside the disc $D(0, R)$. See the right plot in Figure 4 for the resulting reconstruction. We remark that the relative error given by the regularized method is 12% as seen in the top row of Figure 2, while the Born approximation gives 23% at best.

6. ACKNOWLEDGEMENTS

The authors thank Prof. Dr. Sergei V. Pereverzyev and Prof. Dr. Ronny Ramlau for helpful discussions about regularization theory. The work of ML and SS was supported by the Academy of Finland (Finnish Centre of Excellence in Inverse Problems Research). The work of JM was supported by the National Science Foundation under Grant No. 0513509. During part of the preparation of this work, KK worked at the Department of Mathematical Sciences, Aalborg University, Denmark; and SS worked as professor at the Department of Mathematics of Tampere University of Technology, Finland.

REFERENCES

- [1] K. Astala and L. Päivärinta, Calderón's inverse conductivity problem in the plane, *Ann. of Math.* **163** (2006), 265–299.
- [2] K. Astala, M. Lassas and L. Päivärinta, Calderón's inverse problem for anisotropic conductivity in the plane, *Comm. Partial Differential Equations* **30** (2005), 207–224.

- [3] K. Astala, M. Lassas, and L. Päivärinta, Limits of visibility and invisibility for Calderón's inverse problem in the plane, in preparation.
- [4] J. A. Barceló, T. Barceló and A. Ruiz, Stability of the Inverse Conductivity Problem in the Plane for Less Regular Conductivities, *J. Differential Equations* **173** (2001), 231–270.
- [5] T. Barceló and D. Faraco and A. Ruiz Stability of Calderón inverse conductivity problem in the plane *J. Math. Pures Appl.* **88** (2007), 522–556.
- [6] R. Beals and R. Coifman, Scattering, spectral transformations and nonlinear evolution equations. II, Goulaouic-Meyer-Schwartz Seminar, 1981/1982, Exp. No. XXI, (1982).
- [7] R. Beals and R. Coifman, Multidimensional inverse scatterings and nonlinear partial differential equations, in *Pseudodifferential operators and applications (Notre Dame, Ind., 1984)*, 45–70, Proc. Sympos. Pure Math., **43**, Amer. Math. Soc., Providence, RI, 1985.
- [8] J. Bikowski Electrical Impedance Tomography Reconstructions in Two and Three Dimensions; from Calderón to Direct Methods *PhD thesis, Colorado State University, Fort Collins, CO*, (2008).
- [9] N. Bissantz, T. Hohage, and A. Munk. Consistency and rates of Convergence of Nonlinear Tikhonov regularization with random noise, *Inverse Problems* **20** (2004), 1773–1791.
- [10] L. Borcea, Electrical impedance tomography, *Inverse Problems* **18** (2002), 99–136.
- [11] R. Brown Global uniqueness in the impedance-imaging problem for less regular conductivities. (English summary) *SIAM J. Math. Anal.* **27** (1996), 1049–1056.
- [12] B. H. Brown and A. D. Seagar. Applied potential tomography: possible clinical applications. *Clin. Phys. Physiol. Meas.* **6**, 2, (1985), 109–21.
- [13] R. Brown and R. Torres, Uniqueness in the inverse conductivity problem for conductivities with $3/2$ derivatives in L^p , $p > 2n$, *J. Fourier Analysis Appl.*, **9** (2003), 1049–1056.
- [14] R. M. Brown and G. Uhlmann, Uniqueness in the inverse conductivity problem for nonsmooth conductivities in two dimensions, *Comm. Partial Differential Equations* **22** (1997), 1009–1027.
- [15] M. Brühl and M. Hanke, Numerical implementation of two non-iterative methods for locating inclusions by impedance tomography, *Inverse Problems* **16** (2000), 1029
- [16] A. Bukhgeim, Recovering the potential from Cauchy data in two dimensions, *J. Inverse Ill-Posed Probl.*, **16** (2008), 19–34.
- [17] A. P. Calderón, On an inverse boundary value problem, *In Seminar on Numerical Analysis and its Applications to Continuum Physics, Soc. Brasileira de Matemática* (1980), 65–73.
- [18] M. Cheney, D. Isaacson and J. C. Newell, Electrical Impedance Tomography, *SIAM Review* **41** (1999), 85–101.
- [19] H. Cornean, K. Knudsen, and S. Siltanen. Towards a D-bar reconstruction method for three-dimensional EIT. *Journal of Inverse and Ill-posed Problems* **12** (2006), 111–134.
- [20] D. Dos Santos Ferreira, C. Kenig, J. Sjöstrand and G. Uhlmann, Determining the Magnetic Schrödinger Operator from Partial Cauchy Data. *Comm. Math. Phys.* **271** (2007), 467–488.
- [21] D. Freimark, M. Arad, R. Sokolover, S. Zlochiver, and S. Abboud. Monitoring lung fluid content in CHF patients under intravenous diuretics treatment using bio-impedance measurements. *Physiol. Meas.* **28** (2007), S269–S277.
- [22] H. Engl, M. Hanke and A. Neubauer, Regularization of Inverse Problems, *Springer* (2000).
- [23] L. Faddeev, The inverse problem in the quantum theory of scattering. II. (Russian) *Current problems in mathematics* **3** (1974), 93–180.
- [24] I. Frerichs, J. Hinz, P. Herrmann, G. Weisser, G. Hahn, T. Dudykevych, M. Quintel, G. Hellige. Detection of local lung air content by electrical impedance tomography compared with electron beam CT. *J. Appl. Physiol.* **93**, 2, (2002) ,660–6.
- [25] I. Frerichs, J. Hinz, P. Herrmann, G. Weisser, G. Hahn, M. Quintel, G. Hellige. Regional lung perfusion as determined by electrical impedance tomography in comparison with electron beam CT imaging. *IEEE Trans. Med. Imaging* **21** (2002), 646–652.
- [26] I. Frerichs, G. Schmitz, S. Pulletz, D. Schädler, G. Zick, J. Scholz, and N. Weiler. Reproducibility of regional lung ventilation distribution determined by electrical impedance tomography during mechanical ventilation. *Physiol. Meas.* **28** (2007), 261–267.
- [27] A. Greenleaf, Y. Kurylev, M. Lassas, G. Uhlmann: Full-wave invisibility of active devices at all frequencies, *Comm. Math. Phys.* **275** (2007), 749–789.
- [28] A. Greenleaf, Y. Kurylev, M. Lassas, G. Uhlmann, Cloaking Devices, Electromagnetic Wormholes and Transformation Optics. To appear in *SIAM Review*.

- [29] A. Greenleaf, M. Lassas, and G. Uhlmann, The Calderón problem for conormal potentials, I: Global uniqueness and reconstruction, *Comm. Pure Appl. Math* **56** (2003), 328–352.
- [30] A. Greenleaf, M. Lassas, and G. Uhlmann, Anisotropic conductivities that cannot be detected in EIT, *Physiol. Meas.* (special issue on Impedance Tomography), **24** (2003), 413–420.
- [31] A. Greenleaf, M. Lassas, and G. Uhlmann, On nonuniqueness for Calderón’s inverse problem, *Math. Res. Lett.* **10**, 5–6, (2003), 685–693.
- [32] A. Greenleaf, M. Lassas, and G. Uhlmann, Invisibility and inverse problems *Bull. Amer. Math. Soc.* **46** (2009), 55–97.
- [33] M. Hanke Regularizing properties of a truncated Newton-CG algorithm for nonlinear inverse problems *Numer. Funct. Anal. Optim.* **18** (1997), 971–93.
- [34] B. Hofmann, B. Kaltenbacher, C. Pöschl and O. Scherzer A convergence rates result for Tikhonov regularization in Banach spaces with non-smooth operators. *Inverse Problems* **23** (2007), 987–1010.
- [35] T. Hohage and M. Pricop. Nonlinear Tikhonov regularization in Hilbert scales for inverse boundary value problems with random noise. *Inverse Problems and Imaging* **2** (2008), 271–290.
- [36] N. Hyvönen, Complete electrode model of electrical impedance tomography: approximation properties and characterization of inclusions. *SIAM J. Appl. Math.* **64** (2004), 902–931.
- [37] T. Ide, H. Isozaki, S. Nakata, S. Siltanen, and G. Uhlmann, Probing for electrical inclusions with complex spherical waves. *Communications on Pure and Applied Mathematics* **60** (2007), 1415–1442.
- [38] M. Ikehata and S. Siltanen, Numerical method for finding the convex hull of an inclusion in conductivity from boundary measurements, *Inverse Problems* **16** (2000), 1043–1052.
- [39] M. Ikehata and S. Siltanen, Electrical impedance tomography and Mittag-Leffler’s function, *Inverse Problems* **20** (2004), 1325–1348.
- [40] M. Ikehata and S. Siltanen, Numerical solution of the Cauchy problem for the stationary Schrödinger equation using Faddeev’s Green function, *SIAM Journal of Applied Mathematics* **64**, 6, (2004), 1907–1932.
- [41] D. Isaacson, J. L. Mueller, J. C. Newell, and S. Siltanen, Reconstructions of chest phantoms by the D-bar method for electrical impedance tomography, *IEEE Trans. Med. Im.* **23** (2004), 821–828.
- [42] D. Isaacson, J. L. Mueller, J. C. Newell, and S. Siltanen, Imaging cardiac activity by the D-bar method for electrical impedance tomography, *Physiological Measurement* **27** (2006), S43–S50
- [43] L. Justen and R. Ramlau A non-iterative regularization approach to blind deconvolution. *Inverse Problems* **22** (2006), 771–800
- [44] B. Kaltenbacher, A. Neubauer and O. Scherzer, Iterative Regularization Methods for Non-linear Ill-posed Problems, Walter de Gruyter & Co 2008.
- [45] B. Kaltenbacher and A. Neubauer, Convergence of projected iterative regularization methods for nonlinear problems with smooth solutions, *Inverse Problems* **22** (2006), 1105–1119.
- [46] T. Kato, Perturbation theory for linear operators, Springer 1966.
- [47] C.E. Kenig, J. Sjöstrand and G. Uhlmann, The Calderón problem with partial data, *Annals of Math.* **165** (2007), 567–591.
- [48] S. Kindermann and A. Neubauer, On optimal convergence rates for Tikhonov regularization in L^p spaces, submitted, 2008.
- [49] A. Kirsch, An introduction to the mathematical theory of inverse problems, Springer (1996).
- [50] K. Knudsen, On the Inverse Conductivity Problem, *Ph.D. thesis*, Department of Mathematical Sciences, Aalborg University, Denmark (2002)
- [51] K. Knudsen, A new direct method for reconstructing isotropic conductivities in the plane, *Physiol. Meas.* **24** (2003), 391–401.
- [52] K. Knudsen, M. Lassas, J. L. Mueller and S. Siltanen, Reconstructions of piecewise constant conductivities by the D-bar method for electrical impedance tomography, *Proceedings of Applied Inverse Problems 2007, Vancouver*, in press.
- [53] K. Knudsen, M. Lassas, J. L. Mueller and S. Siltanen, D-bar method for electrical impedance tomography with discontinuous conductivities, *SIAM J. Appl. Math.* **67** (2007), 893–913.
- [54] K. Knudsen, J. L. Mueller and S. Siltanen, Numerical solution method for the dbar-equation in the plane, *J. Comp. Phys.* **198** (2004), 500–517.

- [55] K. Knudsen and M. Salo, Determining nonsmooth first order terms from partial boundary measurements, *Inverse Problems and Imaging* **1** (2007), 349–369
- [56] K. Knudsen and A. Tamasan, Reconstruction of less regular conductivities in the plane, *Comm. Partial Differential Equations* **29** (2004), 361–381.
- [57] R. Kohn, H. Shen, M. Vogelius, and M. Weinstein, Cloaking via change of variables in electrical impedance tomography, *Inverse Problems* **24** (2008), 015016.
- [58] P. W. Kunst, S. h. Bohm, G. Vazquez de Anda, M. B. Amato, B. Lachmann, P. E. Postmus, P. M. de Vries. Regional pressure volume curves by electrical impedance tomography in a model of acute lung injury, *Crit. Care Med.* **28**, 1, (2000) 178–183.
- [59] P. W. Kunst, G. Vazquez de Anda, S. H. Bohm, T. J. Faes, B. Lachmann, P. E. Postmus, P. M. de Vries. Monitoring of recruitment and derecruitment by electrical impedance tomography in a model of acute lung injury. *Crit. Care Med.* **28**, 12, (2000), 3891-5.
- [60] P. W. Kunst, A. Vonk Noordegraaf, E. Raaijmakers, J. Bakker, A. B. Groeneveld, P. E. Postmus, P. M. de Vries. Electrical impedance tomography in the assessment of extravascular lung water in noncardiogenic acute respiratory failure. *Chest* **116** (1999), 1695–1702.
- [61] M. Lassas, M. Taylor, and G. Uhlmann, The Dirichlet-to-Neumann map for complete Riemannian manifolds with boundary, *Comm. Geom. Anal.* **11** (2003), 207–222.
- [62] A. Lechleiter, A regularization technique for the factorization method, *Inverse Problems* **22** (2006), 1605–1625.
- [63] A. Lechleiter and A. Rieder, Newton regularizations for impedance tomography: convergence by local injectivity, *Inverse Problems* **24** (2008), 1–18.
- [64] L. Liu, Stability Estimates for the Two-Dimensional Inverse Conductivity Problem, *Ph.D. thesis*, University of Rochester, 1997.
- [65] S. Lu, S. V. Pereverzev, and R. Ramlau, An analysis of Tikhonov regularization for nonlinear ill-posed problems under a general smoothness assumption *Inverse Problems* **23**, 1, 217–230.
- [66] P. Mathé and B. Hofmann, How general are general source conditions? *Inverse Problems* **24** (2008)
- [67] J. L. Mueller and S. Siltanen, Direct reconstructions of conductivities from boundary measurements, *SIAM J. Sci. Comp.* **24** (2003), 1232–1266.
- [68] J. L. Mueller, S. Siltanen, and D. Isaacson. A direct reconstruction algorithm for electrical impedance tomography. *IEEE Trans. Med. Im.* **21** 6, (2002), 555–559.
- [69] E. Murphy, J. L. Mueller, and J. C. Newell. Reconstruction of conductive and insulating targets using the D-bar method on an elliptical domain. *Physiol. Meas.* **28** (2007), S101–S114.
- [70] A. I. Nachman. Reconstructions from boundary measurements. *Ann. of Math.* **128** (1988), 531–576.
- [71] A. I. Nachman, Global uniqueness for a two-dimensional inverse boundary value problem, *Ann. of Math.* **143** (1996), pp. 71–96.
- [72] A. I. Nachman, Global uniqueness for a two-dimensional inverse boundary value problem *University of Rochester, Dept. of Mathematics Preprint Series* **19** (1993).
- [73] J. C. Newell, R. S. Blue, D. Isaacson, G. J. Saulnier, and A. S. Ross. Phasic three-dimensional impedance imaging of cardiac activity. *Physiol. Meas.* **23** (2002), 203–209.
- [74] R. G. Novikov A multidimensional inverse spectral problem for the equation $-\Delta\psi + (v(x) - Eu(x))\psi = 0$, *Funktsional. Anal. i Prilozhen.* **22** 11–22 (transl.) *Funct. Anal. Appl.* **22** (1988), 263–272.
- [75] L. Päivärinta, A. Panchenko, and G. Uhlmann, Complex geometrical optics for Lipschitz conductivities, *Rev. Mat. Iberoam.* **19** (2003), 57–72.
- [76] R. Ramlau. Regularization properties of Tikhonov regularization with sparsity constraints. *ETNA* **30** (2008), 54–74.
- [77] R. Ramlau and G. Teschke. A Tresholding Iteration for Nonlinear Operator Equations with Sparsity Constraints. *Numerische Mathematik* **104**, 2, (2006), 177–203.
- [78] E. Resmerita. Regularization of ill-posed problems in Banach spaces: convergence rates, *Inverse Problems* **21** (2005), 1303–1314.
- [79] L. Rondi, *On the regularization of the inverse conductivity problem with discontinuous conductivities*, *Inverse Problems and Imaging* **2** (2008), 397–409.
- [80] M. Salo Semiclassical pseudodifferential calculus and the reconstruction of a magnetic field *Comm. Partial Differential Equations* **31** (2006), 1639–1666.

- [81] S. Siltanen Electrical impedance tomography and Faddeev Green's functions, *Ann. Acad. Sci. Fenn. Mathematica Dissertationes* **121** (1999).
- [82] S. Siltanen, J. Mueller and D. Isaacson, An implementation of the reconstruction algorithm of A. Nachman for the 2-D inverse conductivity problem, *Inverse Problems* **16** (2000), 681–699. (Erratum: *Inverse problems* **17**, 1561-1563)
- [83] S. Siltanen, J. Mueller, and D. Isaacson Reconstruction of High Contrast 2-D Conductivities by the Algorithm of A. Nachman., In *AMS proceedings of the 2000 conference on Radon Transforms and Tomography*, Contemporary Mathematics 278, (2001), E. Quinto, editor, 241–254.
- [84] H. Smit, A. Vonk Noordegraaf, J. T. Marcus, A. Boonstra, P. M. de Vries, and P. E. Postmus. Determinants of pulmonary perfusion measured by electrical impedance tomography. *Eur. J. Appl. Physiol.* **92** (2004), 45–49.
- [85] Z. Sun and G. Uhlmann, Anisotropic inverse problems in two dimensions, *Inverse Problems* **19** (2003), 1001–1010.
- [86] J. Sylvester, An anisotropic inverse boundary value problem, *Comm. Pure Appl. Math.* **43** (1990), 201–232.
- [87] J. Sylvester and G. Uhlmann. A global uniqueness theorem for an inverse boundary value problem. *Ann. of Math.* **125** (1987), 153–169.
- [88] G. Uhlmann and J-N. Wang, Complex geometrical optics solutions and reconstruction of discontinuities *SIAM J. Appl. Math.* **68** (2008), 1026–1044.
- [89] I. N. Vekua, Generalized Analytic Functions, *Pergamon Press* (1962).
- [90] J. A. Victorino, J. B. Borges, V. N. Okamoto, G. F. J. Matos, M. R. Tucci, M. P. R. Carames, H. Tanaka, D. C. B. Santos, C. S. V. Barbas, C. R. R. Carvalho, M. B. P. Amato. Imbalances in Regional Lung ventilation: a validation study on electrical impedance tomography. *Am. J. Respir. Crit. Care Med.* **169** (2004), 791–800.
- [91] K. Yoshida, Functional analysis, Springer 1966
- [92] S. Zlochiver, M. M. Radai, D. Barak-Shinar, H. Krief, T. Ben-Gal, V. Yaari, R. Ben-Yehuda, B. Strasberg, S. Abboud. An EIT system for monitoring lung conductivity in CHF patients. www.cardio-inspect.com/EIT_System.pdf.

DEPARTMENT OF MATHEMATICS, TECHNICAL UNIVERSITY OF DENMARK
E-mail address: `k.knudsen@mat.dtu.dk`

DEPARTMENT OF MATHEMATICS AND STATISTICS, UNIVERSITY OF HELSINKI, FINLAND
E-mail address: `matti.lassas@helsinki.fi`

DEPARTMENT OF MATHEMATICS AND SCHOOL OF BIOMEDICAL ENGINEERING, COLORADO STATE UNIVERSITY, FORT COLLINS, CO, USA
E-mail address: `mueller@math.colostate.edu`

DEPARTMENT OF MATHEMATICS AND STATISTICS, UNIVERSITY OF HELSINKI, FINLAND
E-mail address: `samuli.siltanen@helsinki.fi`

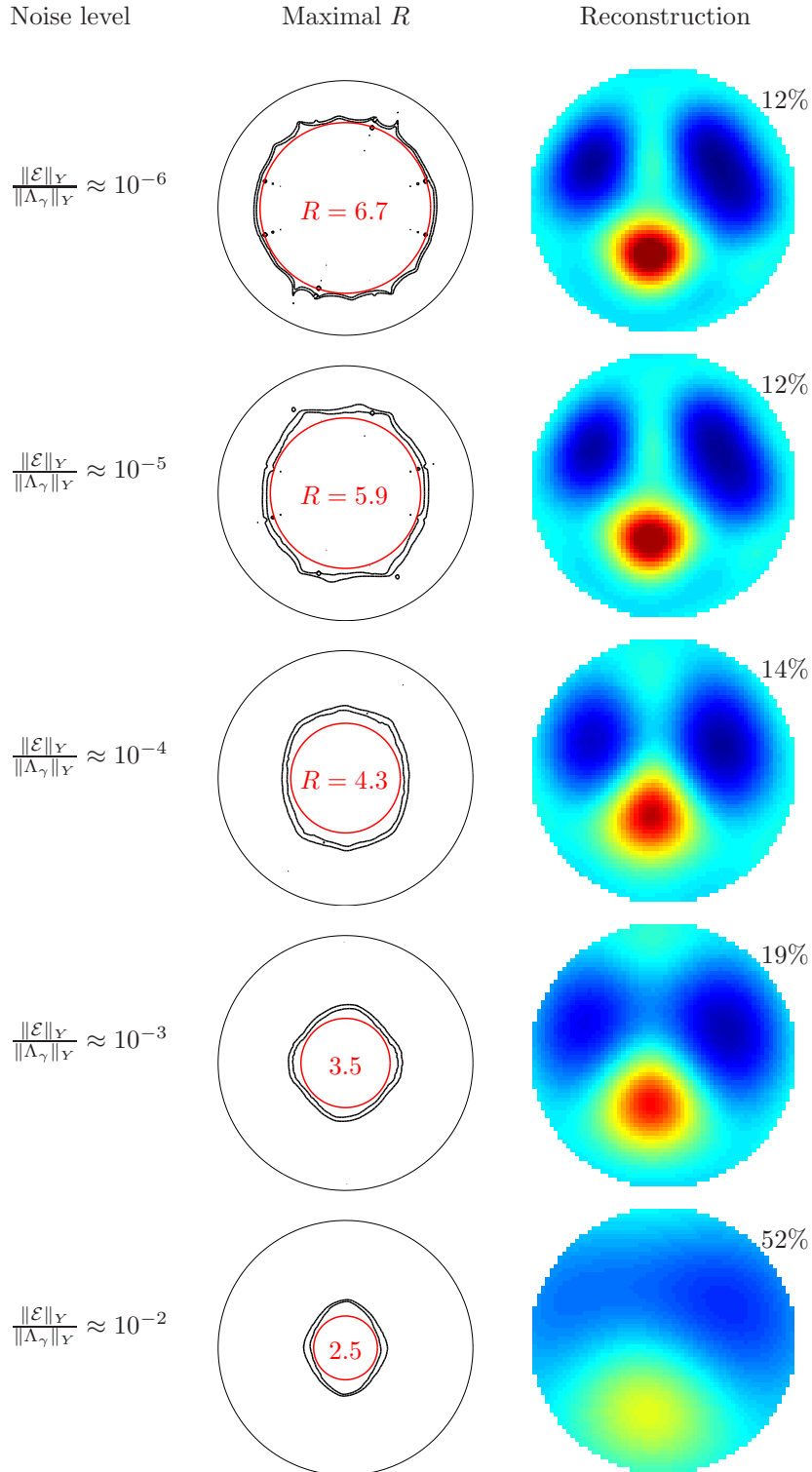


FIGURE 2. Reconstructions with various noise levels. In the column “Maximal R ” the large circle has radius 10, and inside the irregular curves the scattering data $\mathbf{t}^{\text{BIE}}(k)$ has reasonable accuracy. The percentages shown are relative L^2 errors of the reconstructions. The color scale of all the reconstructions is the same.

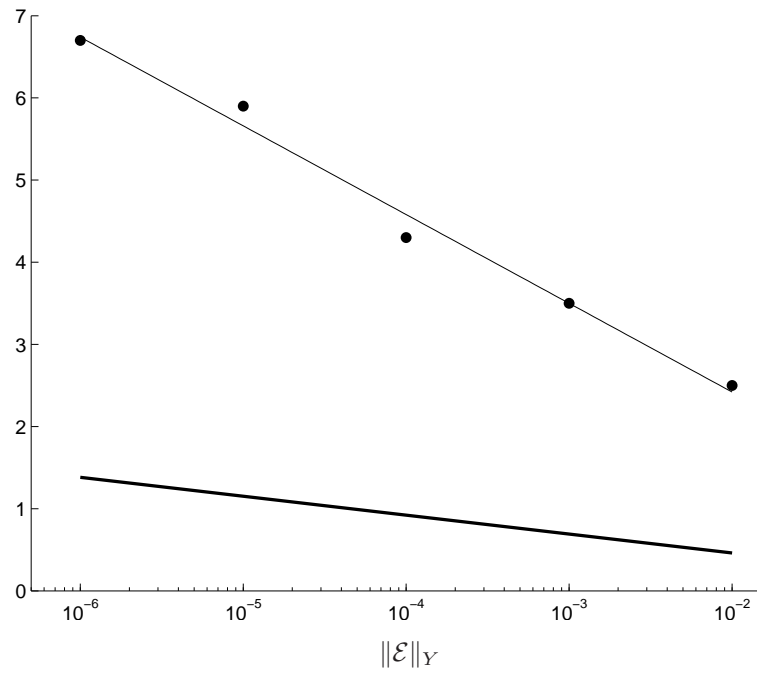


FIGURE 3. Quantitative comparison of observed and predicted truncation radii. Thick line has slope -0.1 and shows the theoretical truncation radius $R = -\frac{1}{10} \log \varepsilon$. Black dots indicate the empirical truncation radii given in Figure 2. Thin line is a linear least squares fit to the data points; its slope is -0.47 . Thus the practical algorithm performs better than predicted by the theory.

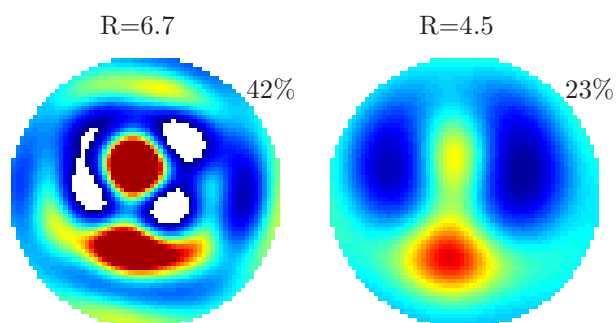


FIGURE 4. Reconstructions using the Born approximation (5.2) and noise level $\|\mathcal{E}\|_Y \approx 10^{-6}$ and two choices of truncation radius: $R = 6.7$ (left plot) and $R = 4.5$ (right plot). The percentages shown are relative L^2 errors of the reconstructions. The color scale of both reconstructions is the same as in Figure 2; the white spots in the left plot denote regions where reconstructed values exceed the interval $[0.4, 2]$.